TUNING THE PROPERTIES OF INJECTABLE *IN SITU* GELLING POEGMA HYDROGELS BY CONTROLLING PRECURSOR POLYMER MOLECULAR WEIGHT AND STRUCTURE

TUNING THE PROPERTIES OF INJECTABLE *IN SITU* GELLING POEGMA HYDROGELS BY CONTROLLING PRECURSOR POLYMER MOLECULAR WEIGHT AND STRUCTURE

By

IVAN UROSEV

A Thesis Submitted to the School of Graduate Studies in Partial Fulfillment of the

Requirements for the Degree Master of Applied Science

McMaster University © Copyright by Ivan Urosev, May 2016

MASTER OF APPLIED SCIENCE (2016) McMaster University

(Biomedical Engineering) Hamilton, Ontario

TITLE: Tuning the properties of injectable *in situ* gelling POEGMA hydrogels by controlling precursor molecular weight and architecture

AUTHOR: Ivan Urosev

SUPERVISOR: Dr. Todd Hoare

NUMBER OF PAGES: xi, 96

Abstract

Injectable hydrogels made from synthetic polymers represent a versatile class of biomaterials that have been extensively investigated for their potential application as drug delivery vehicles and tissue engineering scaffolds, due to their ease of *in vivo* delivery, high tuneability, and across-linked hydrophilic network structure that has mechanical and chemical similarities to native tissues. In the case of injectable hydrogels that are formed via covalent bonds between synthetic polymers, hydrogel properties can often be tuned by chemical modification of the precursor polymers. However, changing the chemistry of a hydrogel system can often have unforeseen or unintended consequences in terms of factors such as drug partitioning or how cells interact with the hydrogel substrate. There is a need, therefore, for devising alternative methods to modulate the properties of hydrogels while maintaining chemical uniformity within the gels. This thesis investigates two methods for modulating the properties of poly(oligoethylene glycol methacrylate) (POEGMA) based injectable hydrogels that work by changing the structural characteristics of the POEGMA precursors while maintaining uniformity of chemical factors such as functional group distribution. POEGMA is a widely used synthetic poly(ethylene glycol) analogue that has a number of beneficial properties including being biodegradable, non-cytotoxic, and readily functionalizable. In the first method, the properties of POEGMA-based hydrogels were modulated by changing the molecular weight of the POEGMA precursors that were used to form the gels. Well-defined functionalized POEGMA polymers of various molecular weights (with complementary hydrazide/aldehyde functionalities) were prepared using RAFT

polymerization, and the polymers were subsequently mixed to form hydrogels *in situ* via rapid formation of hydrazine bonds. These gels were assessed to determine how polymer molecular weight affects properties such as mechanical strength, swelling/degradation, and gelation kinetics. In the second method, hyperbranched POEGMA polymers were prepared by inclusion of a di-vinyl cross-linker into the RAFT polymerization of these polymers. A series of functionalized polymers was prepared by varying the degree of branching in the polymers, with the properties of these polymers subsequently investigated to determine how branching degree affected polymer properties. The polymers were then demonstrated to be capable of forming hydrogels *in situ*. Overall, by applying chemistry-driven approaches to engineer defined structures in the precursor components of hydrogels, gels with well-defined and tunable properties that are directly related to the structure of those precursor polymers can be achieved, permitting the preparation of injectable hydrogels with highly analogous chemistries but different bulk properties.

Acknowledgements

I would first like to thank my supervisor Dr. Todd Hoare for his measured advice and continuing support, and particularly for giving me the opportunity to discover a career that I can pursue for the rest of my working life. I applied to the Master's program at McMaster at a time when I had few defined plans for the future and, because Dr. Hoare gave me a chance where others might not have, I am leaving the program with a sense of purpose that I was sorely lacking, so for that I will always be grateful.

I would also like to thank my other mentors in the lab, particularly Drs. Niels Smeets and Lukas Sadowski, for their sage advice, and for patiently entertaining my sometimes elementary questions. Additionally, I would like to thank all of the members of the Hoare lab, for helping me find my way when I was getting started, and for making it fun to come into work everyday. Special thanks go out to Helen Dorrington, for her assistance with the experiments and figures for chapter 4 of this thesis and for putting up with my often-onerous requests, Maryam Badv, for her assistance with experiments for chapter 3, and Donovan Ramkishun. Extra special thanks go out to Emilia Bakaic, who has looked out for me since the day that I started in the lab. Thanks for helping to keep me sane for two years.

Finally, and most importantly, thanks to my family and in particular my parents Vesna, Stojan, and Kevin. Their monastic patience and unshakeable support have allowed me to succeed to the extent that I have, often in spite of myself. I hope that I can continue to live up to the opportunities that they have provided for me in the future.

Table of Contents

List of Figures

List of Tables

List of Abbreviations and Symbols

AA – Acrylic Acid
ADA – Aminoacetaldehdye dimethyl acetal
ADH – Adipic acid dihydrazide
AIBN - Azobisisobutyronitrile
ATRP – Atom transfer radical polymerization
BSA – Bovine Serum Albumin
CPCDB – 2- cyano-2-propyl 4-cyanobenzodithioate
CRP – Controlled Radical Polymerization
DB – Degree of Branching
DCM – Dichloromethane
DIW – Deionized water
DMEM – Dulbecco's modified Eagle medium (high glucose, high pyruvate)
ECM – Extracellular Matrix
EDC – N'-ethyl-N-(3-dimethylaminopropyl)-carbodiimide
EGDMA – Ethylene glycol dimethacrylate
HA – Hyaluronic Acid
LCST – Lower Critical Solution Temperature
LVE – Linear Viscoelastic Region
MAA – Methacrylic acid
$M(EO)_2MA$ – Di(ethylene glycol) methyl ether methacrylate
MW – Molecular Weight
NMR – Nuclear magnetic resonance
PDI – Polydispersity Index
PEG – poly(ethylene glycol)
PHEMA – poly(2-hydroxyethyl methacrylate)
PNIPAM – poly(N-isopropylacrylamide)
POEGMA – poly(oligoethylene glycol methyl ether methacrylate)
RAFT – Reversible Addition-Fragmentation chain Transfer
RC – Regenerated cellulose
RGD – peptide/binding motif; Arginine, Glycine, Aspartic Acid
SEC – Size-exclusion chromatography
VPTT – Volume Phase Transition Temperature
5-FITC – 5-Fluorescence isothiocyanate
5-FTSC - fluorescein-5-thiosemicarbazide

1 Introduction

The challenges associated with the design of biomaterials are broad, as the conditions under which these biomaterials are to be used can vary widely. Biomaterials are needed for the *in vitro* modeling of various pathologies, for the delivery of various kinds of drugs over long time frames, and for the construction of scaffolds for tissue engineering, among many other applications. In the context of these varied applications, biomaterials will need to be able to endure a range of physical conditions (i.e. pH, temperature), intense physical stress (i.e. at the site of knee joints), and biological stresses in the form of the body's innate immune response. Given these myriad requirements, the notion of a universal biomaterial is probably not a realistic one. However, a general rule of thumb may be that a biomaterial should, as closely as is possible, emulate the healthy properties of the tissue that it is meant to supplement.

Hydrogels are a class of materials that share many similarities with the extracellular matrix (ECM) that cells exist in *in vivo*. These gels are porous networks of cross-linked polymers with the capacity to absorb large quantities of water, much like the collagen networks that form the backbone of the ECM. Furthermore, hydrogels are highly tuneable materials; their mechanical, chemical, and biological properties can be readily modified to emulate particular portions of the *in vivo* environment. Given their biomimetic nature, hydrogels have attracted a great deal of research interest for their potential application as biomaterials in a range of *in vitro* and *in vivo* contexts.

The objective of the work described herein is to produce injectable hydrogels based on poly(Oligoethylene glycol methyl ether methacrylate) (POEGMA) precursors

with a variety of structural characteristics. The aim was to investigate how these varying structural characteristics (in particular, control over the molecular weight and the degree of branching of the precursor polymers) affected the properties of the hydrogels produced from these polymers. Specifically, this work focused on using controlled radical polymerization (CRP) techniques to make polymers, with well-defined sizes and shapes. Chapter 2 of this thesis is a literature review of hydrogels in general, and POEGMA gels in particular. A general review of the use of these biomaterials is given, as well as an update on some recent developments in the field. Chapter 3 describes the process of tuning the moleculr weight (MW) of hydrazide- or aldehyde-functionalized POEGMA polymers to produce precursor polymers with a range of molecular weights. These precursors were then combined with other, complimentary precursors in various combinations to produce hydrogels; the mechanical and physical characteristics of these hydrogels were subsequently assessed to determine how they were affected by the variation in size of the precursors that composed them. Chapter 4 focuses on using CRP to produce hyperbranched polymers in a controlled and reproducible manner. These polymers were prepared with varying degrees of branching and were subsequently used to produce hydrogels with linear polymers containing complimentary functionalities. The structural and physical properties of these hyperbranched polymers were assessed in relation to linear controls to determine what role hyperbranching plays in the behavior of POEGMA polymers. Together, the results from these chapters are used to draw conclusions about how the physical and structural properties of POEGMA

polymers can be modulated to produce biomaterials with a variety of desirable properties.

2 Literature Review

2.1 Injectable hydrogels for biomedical applications

2.1.1 Overview

Hydrogels are three-dimensional networks of cross-linked natural or synthetic polymers; these polymers can be arrayed in various combinations to produce a range of characteristics. By altering such parameters as cross-linking density, monomer composition, and polymer chain length, hydrogels can be tuned to exhibit properties that are appropriate for various targeted applications [1]. All hydrogels, however, have a number of generally conserved properties that make them attractive for use in a biomedical context; namely, they are hydrophilic, porous, and able to absorb large quantities of water. Other features that are commonly desirable in hydrogels (but that are not necessarily universal) include biocompatibility, degradability *in vivo*, and anti-fouling capability. Together, these properties allow hydrogels to mimic soft living tissues better than any other synthetic biomaterial [2].

Given their biomimetic nature, hydrogels have the potential for use in such varying capacities as wound healing, drug delivery, tissue engineering, etc. [1]. An investigation of the use of hydrogels in these contexts is given in the subsequent subsections. The examples below are intended to illustrate the breadth of potential hydrogel applications, and they are far from comprehensive. Furthermore, as the

complement of available monomers continues to grow, and as more advanced methods for gel formation are demonstrated, it can be expected that the potential range of hydrogel applications will continue to expand in tandem.

2.1.2 Hydrogels as drug delivery vehicles

Hydrogels have attracted a great deal of attention as potential vehicles for drug delivery. Their porous structure, and highly tuneable physical and chemical properties allow hydrogels to be tailored to release a wide variety of drugs over different time frames and in different *in vivo* environments [3]. The major benefit of using hydrogels as drug delivery vehicles is likely a pharmacokinetic one; that is, using a hydrogel reservoir to slowly release a drug over time (usually by diffusion of the drug through the porous gel network, and/or degradation of the gel over time) theoretically produces a more stable steady-state concentration of a drug over time, as compared to the wide variation in drug concentration that is typical of more traditional methods of drug delivery like direct intravenous injection or oral administration[4]. Other benefits that hydrogels provide in a drug delivery context include biocompatibility, a high capacity for drug loading, and the potential to respond to environmental factors (i.e. pH, temperature) which can be used for targeted drug release [3].

To-date, hydrogel-based drug delivery vehicles have been developed in a variety of formats, including nanoparticles, contact lenses, and premade bulk reservoirs [5]. The latter system has been further improved by the development of injectable bulk hydrogels, which form from cross-linking polymers *in situ*, eliminating the need for costly and potentially dangerous surgical implantation. As an example, one particular

area in which hydrogels have achieved broad (even clinical) application is in the field of soft contact lenses for drug delivery. Recent publications describe a wide variety of hydrogel-based drug delivery constructs, ranging from thermosensitive calcium alginate microspheres for enzyme release [6], to nanocomposite hydrogels composed of 3D-polymers and nanoparticles [7]. Given the favourable release profiles that can be achieved from hydrogel reservoirs, it is certain that hydrogels will continue to garner intensive research focus for a growing variety of drug delivery applications.

2.1.3 Hydrogels for tissue engineering

Another context in which hydrogels have been shown to have broad potential for application is that of scaffolds for tissue engineering. As described above, hydrogels have a morphology and hydophilicity that closely mimics native tissues. Furthermore, the flexibility of hydrogels in terms of their chemical functionality, means that they provide a platform that can be readily tailored to interact with a variety of different cell types, in a variety of *in vitro* or *in vivo* environments [8]. *In vitro*, hydrogels can be used to support the growth of cells that are not able to grow (or grow while maintaining their functionality) on more standard substrates (i.e. polystyrene), such as certain types of stem cells [9]. In fact, the functionality and physical properties of hydrogels can be tailored to direct stem cell behavior over time. Factors such as substrate mechanical properties [10] and the presence of surface functional groups [11] have been modulated to direct how stem cells grow and differentiate on or within hydrogel scaffolds. Additionally, hydrogels can be used to provide a model of the *in vivo* environment, in order to better study cell behavior, or the progression of certain pathologies. Notable

examples include a vascularized matrigel chip that can mimic the electrophysiological behavior of cardiomyocytes in a petri dish [12], and a polyester-based scaffold that was used to model the microenvironment around certain types of tumors, in order to more accurately track how these tumors might respond to various chemotherapies *in vivo* [13].

In vivo hydrogel scaffolds are most often used to support the growth of certain cell types that have therapeutic potential, or to protect implanted cells from the body's immune system by masking them in 3-dimensional constructs that resist protein adhesion[14]. Another approach has been to create hybrids of hydrogels and more traditional implantable materials, in order to achieve synergistic tissue engineering constructs that can be used in a variety (particularly high-stress) *in vivo* environments. For example, much work has been done in using hydrogels to modify the bioactivity of traditionally bio-inert implant materials (i.e. ceramics, metals), so that they might better reflect the *in vivo* behavior of natural tissues. In 2015, Seol and colleagues investigated the efficacy of hydrogel-ceramic composite materials in promoting the regeneration of articular cartilage. The team implanted their hydrogel-ceramic composite at the site of osteochondral defects in rabbit knee joints, and they were able to show that the composite acted synergistically to promote regeneration of cartilage at the implant site [15].

2.1.4 Injectable hydrogel systems

As might be expected given their broad range of applications, hydrogels also have the potential for administration via a variety of pathways. Some common methods

for hydrogel administration in a biomedical context include surgical implantation as a bulk gel or adhesive [16], topical application onto wounds or burn sites [17], and ophthalmologically as contact lenses for drug delivery [18]. Of course the preferred method for the clinical administration of a particular hydrogel will depend upon its intended application as well as the physical characteristics (elasticity, method of cross-linking, etc.) of the gel itself. However, all methods of administration (within the context of the intended application of the hydrogel) seek to maximize patient compliance, safety, and precision (i.e. the targeting of the hydrogel to its site of action).

One method that is being explored for its potential to satisfy the above criteria in a broad range of clinical settings is injection. Most often, administration of hydrogels via this method involves the injection of hydrogel precursors that can subsequently cross-link *in situ*, as the physical properties of pre-formed gels preclude their passing through even the lowest gauge needles. Therefore, in order for a gel to be amenable to injection, it must be formed by precursor polymers that can react over the appropriate timescale; that is, not so fast as to initiate gelling while the polymers are being injected, and not so slow as to disperse from the targeted site of action before gelling can occur. To date, a number of cross-linking mechanisms have been used to create injectable systems, including thermal gelation, ionic interactions, photopolymerization, and chemical cross-linking by cross-linking agents [19]. These and other methods of *in situ* cross-linking can be broadly divided into two categories: systems based on physical interactions between polymers and systems based on the formation of covalent bonds [20]. As is the case

with the various other methods of hydrogel administration, the optimal method of *in situ* cross-linking will depend upon the intended application of the gel.

Physical cross-linking *in situ* can either be triggered by the physical/chemical environment at the target site (e.g. by inducing a phase transition in the precursors that leads to their physical interaction) or through latent interactions between the precursors (e.g. electrostatic interactions). These mechanisms have the advantage of not depending upon the presence of reactive functional groups, which can often be incompatible with the chemical environment of the body [21]. However, interactions of this nature are difficult to control with respect to how their strength affects their *in vivo* biodegradability: physical interactions that are too weak will result in the diffusion of the precursors away from the target site before the gel has a chance to form while those that are too strong will preclude degradation in the normal physiological environment [22]. The usefulness of physically cross-linking systems is therefore generally limited to certain shorter-term biomedical applications, and increasingly research focus has shifted to other methods for producing injectable hydrogels.

This review will focus mainly on *in situ* gelling via covalent bond formation, as that is the mechanism that is used to produce the gels that are reported in this thesis. In order for a covalently gelling system to be compatible with application *in vivo*, it should meet the following criteria:

1. The bonding reaction should occur quickly under physiological conditions in order to prevent "leaching away" of precursors.

2. The bonding reaction should occur orthogonally with respect to functional groups which are common *in vivo*, in order to minimize potentially harmful interactions between polymers and native tissues.
3. The cross-linked gel should be degradable over time at a rate that is appropriate for its intended application and will not lead to persistence of the gel in the body beyond its intended period of clinical relevance. The products of this degradation should be non-toxic (for most applications), and they should have a molecular weight (MW) that falls below the kidney clearance threshold (hydrodynamic diameter = 5 – 6 nm)[23].
4. The gel precursors, any associated cross-linkers, the gel itself, and any degradation products should, as much as is possible, avoid eliciting an immune response from the body.

To date, a number of covalent bond forming reactions that meet the above criteria have been applied in the formation of *in situ* gelling hydrogels. A summary of these reactions is given in Figure 2 – 1.

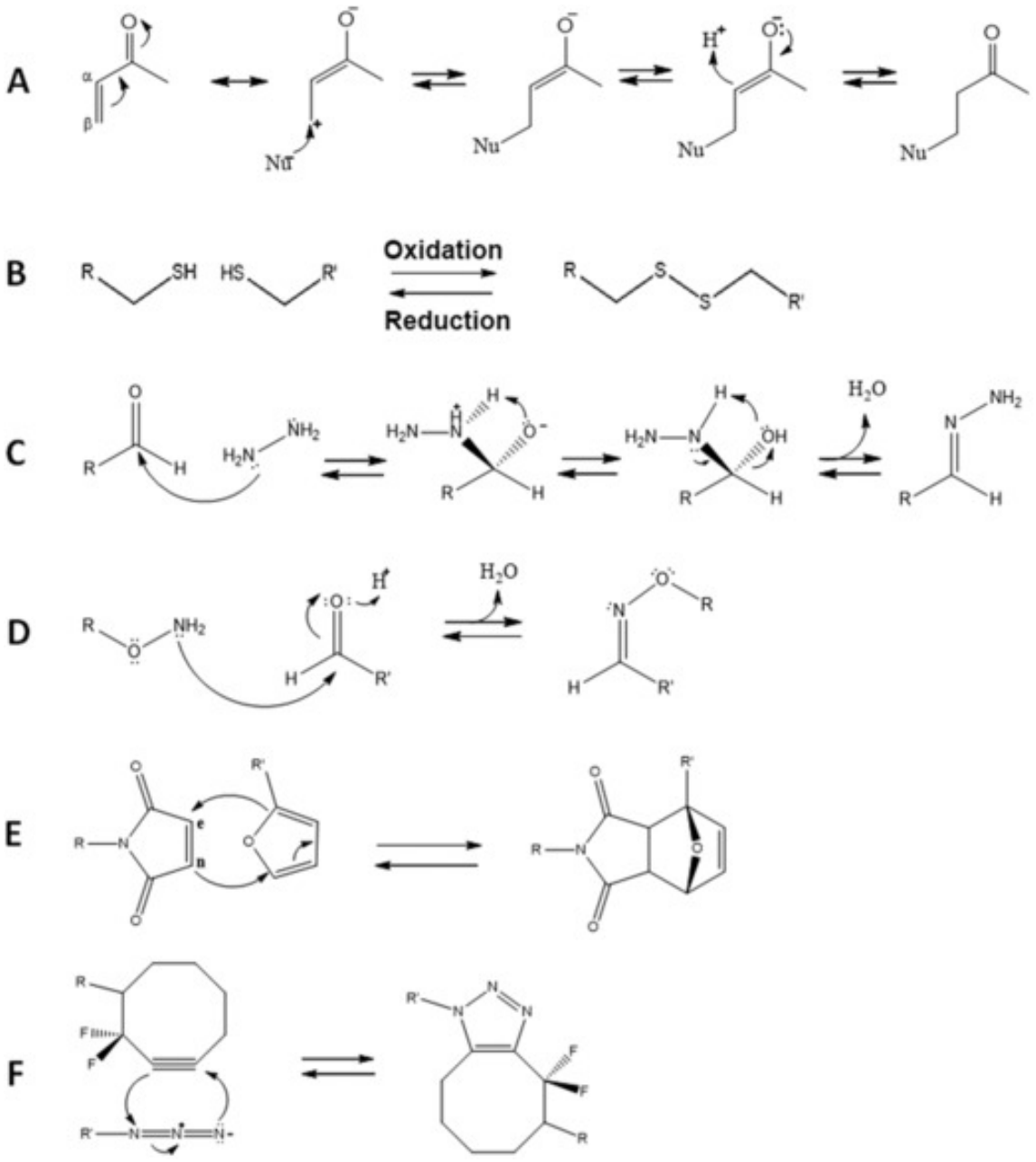

Figure 2 - 1. Covalent bond forming chemistries that are used in the formation of *in situ* gelling hydrogels: (A) 1,4–addition (Michael-type addition); (B) disulfide formation; (C) hydrazone condensation; (D) oxime formation; (E) alkyne-azide 1,3-dipolar Huisgen cycloaddition; (F) Diels-Alder cycloaddition. *Figure adapted from the literature [22]*.

The particular chemistry that is used in a certain injectable hydrogel system will depend upon the intended application of the gel, as the above reactions proceed according to varied reaction kinetics and the bonds produced provide different degrees of stability in different physiological environments. For example, Michael-type addition reactions can typically drive gelation over periods ranging from a few minutes to tens of minutes at physiological pH [24], whereas gelling that is driven by hydrazone condensation may occur over timescales that are on the order of seconds [22]. The latter reaction has been the focus of prolonged investigation by our group, and so it will be highlighted in the remainder of this review.

In hydrazone chemistry, a nucleophilic hydrazine (or a derivative) attacks the electrophilic carbon of a carbonyl group (most often a ketone or aldehyde) to produce a hydrazone bond (a type of Schiff base) while losing a water (Fig. 2 – 1C). Schiff bases formed by the reaction of primary amines and carbonyls are normally very hydrolytically labile [25], but hydrazone bonds show improved stability in water due to the increased nucleophilicty derived from the lone-pair-bearing α-amines (the α-effect) [26]. It should also be noted that due to the high toxicity of hydrazines [27], more physiologically tolerable hydrazides are generally used for this reaction in a biomedical context[22]. As mentioned above, one of the principal advantages of using this type of reaction for hydrogel formation is the rapid kinetics of gelation that can be achieved. Additionally, the hydrolytically labile nature of hydrazone bonds means that gels formed by this method will be readily degradable *in vivo*. The rate of this degradation can be tuned by adjusting the density of hydrazone cross-links in the gel [28] or through the inductive

effects of certain substituted functional groups (i.e. benzenes) adjacent to the hydrazine bond [29]. Given the suitability of this type of chemistry for covalent bond formation in a biomedical context, it is unsurprising that hydrazone condensation has seen widespread application in the production of injectable hydrogels. For example, in 2011 Tan and colleagues cross-linked an aldehyde functionalized hyaluronic acid (HA) derivative with α,β-polyaspartylhydrazide to produce injectable hydrogels for protein delivery. Using this system, they were able to achieve sustained levels of bovine serum albumin (BSA) release, while maintaining low cellular toxicity [30]. In the context of tissue-engineering, Drager and co-workers used hydrazone bond-forming HA and alginate derivatives to produce a matrix for the encapsulation of cardiomyocytes, facilitating the generation of contractile bioartificial cardiac tissue from cardiomyocyte-enriched neonatal rat heart cells [31]. The above examples illustrate the diverse range of injectable hydrogel applications for which hydrazone condensation could be useful, particular given the strong record of cytocompatibility that this chemistry has demonstrated in the literature [32-34].

To date, our group has been able to use hydrazone-bond forming chemistry to produce a variety of injectable hydrogels, such as thermoresponsive poly(N-isopropylacrylamide) (PNIPAM) based gels with low cytotoxicity [35] as well as gels based on the poly(ethylene glycol) (PEG) analogue poly(oligoethylene glycol methyl ether methacrylate) (POEGMA) [36]. This work expands on the use of POEGMA; manipulating the properties of POEGMA-based hydrogels by changing the functional and physical characteristics of their precursors, in a manner that is described below.

2.1.5 POEGMA-based hydrogels

One of the most widely used polymers in the formation of hydrogels for biomedical applications is PEG [37]. PEG has seen such extensive use because it is a hydrophilic, non-cytotoxic material that is able to effectively "hide" exogenous objects from the body's immune system [37]. Furthermore, PEG's hydrophilicity gives it significant anti-fouling capabilities, making it an ideal material for use in applications such as cardiovascular stents [38]. To date, some other biomedical applications of PEG include use in vehicles for gene delivery [39], as a substrate for tissue engineering [40], and as "smart" chemotherapy carriers for the specific targeting of tumors [41]. Despite this prodigious research focus, PEG does suffer a significant drawback in that there is a limited opportunity for functional modification of PEG polymers. This lack of chemical versatility is due to the fact that the only available functional groups on PEG are the functional groups at either end of the molecule. These functional groups tend to be used up in the step-growth polymerizations that are commonly employed to produce PEG polymers; therefore, the only available sites for functionalization of these polymers are the few end-groups that might remain at the ends of polymer chains post-polymerization [42]. Given this short-coming of PEG, significant attention has been dedicated to producing new polymeric biomaterials which share PEG's desirable biological and physical properties but also afford greater opportunities for post-polymerization functionalization [43].

One such PEG analogue is POEGMA. POEGMA has been shown to display protein adhesion repellent properties reminiscent of PEG, while affording greater opportunities

for expanded polymer functionalization [44]. Structurally, POEGMA bears a resemblance to PEG in that it contains the PEG repeat unit within its oligo sidechain (Fig. 2 – 2); however, the OEGMA precursor also contains a methacrylate group that allows for free/controlled radical polymerizations of OEGMA, greatly expanding its chemical functionality by introducing the potential for free radical copolymerization [36]. Researchers have sought to take advantage of this versatility for at least the past decade. Some recent developments in the field of POEGMA-based biomaterials include a disulfide fluorescent probe for tracing intracellular drug delivery [45], protein resistant films for protein separation [46], and a scaffold for vascular tissue engineering [47]. A particularly attractive feature of POEGMA is the phase transition that it displays in water at certain temperatures. The particular transition temperature of POEGMA can be modulated by varying the mole fraction of short-chain and long-chain OEGMA monomers (referring to the length of their ethylene glycol side-chain) that are incorporated into a polymer. In general, it has been found that increasing the proportion of long-chain OEGMA in a POEGMA molecular increases its transition temperature. This is likely due to the hydrophilicity of the ethylene glycol side-chain, which would increase the solubility of the molecule in water [48].

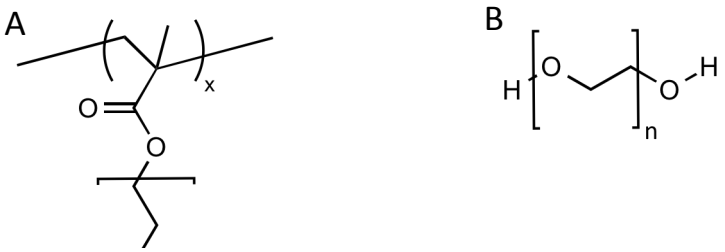

Figure 2 - 2. The chemical structures of (A) POEGMA and (B) PEG.

Our group's major contribution to the field of POEGMA-based hydrogels has been the creation of a system for its injectable delivery. This was achieved via copolymerization of OEGMA, 2-(2-methoxyethoxy) ethyl methacrylate ($M(EO)_2MA$; short-chain OEGMA), and acrylic acid (AA) or N-(2,2-dimethoxyethyl) methacrylamide (DMEMAm) in various ratios. Copolymers containing acrylic acid residues were subsequently functionalized at the carboxylic acid site by N'-ethyl-N-(3-dimethylaminopropyl)-carbodiimide (EDC) mediated coupling of adipic acid dihydrazide, resulting in conversion of the carboxylic acids to hydrazide groups (POEGMA-A). Copolymers containing DMEMAm were functionalized by simple acid deprotection of acetal groups to yield aldehyde functionalized POEGMA (POEGMA-B). Co-extrusion of these polymers through a double-barreled syringe results in rapid cross-linking through the formation of hydrazine bonds, ultimately resulting in gelation [36]. The general scheme for this system is outlined in Figure 2 – 3. By varying the molar ratios of OEGMA and $M(EO)_2MA$ in our polymers, we have been able to control the LCST behavior of both POEGMA polymers and POEGMA-based hydrogels in water [49]. Additionaly, by using techniques such as electrospinning [50] and dip-coating [51] we have been able to produce a variety of POEGMA constructs for various applications (i.e. cell encapsulation

in POEGMA fibers, coating of cellulose paper to produce biosensors). The work reported herein expands on that system to produce injectable POEGMA-based hydrogels with assorted properties and functionalities.

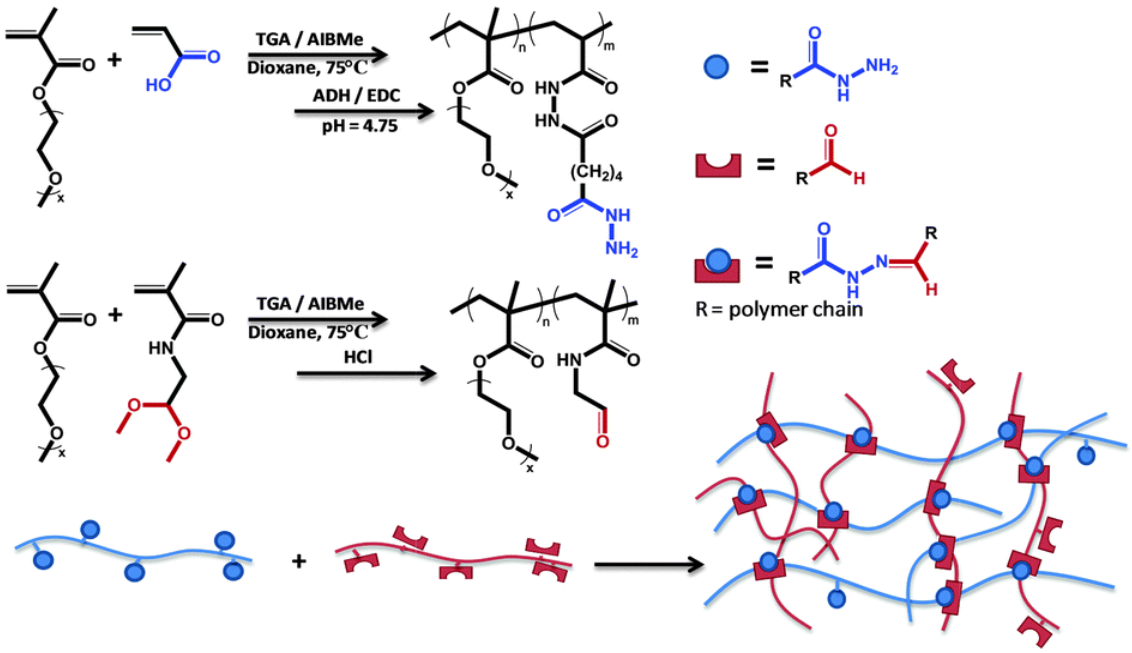

Figure 2 - 3. Scheme for the preparation of aldehyde and hydrazide-functionalized POEGMA precursors, and formation of hydrogels from mixing of these precursors. *Figure adapted from the literature* [36].

2.2 Polymer Synthesis and 3-dimensional Structural Effects

2.2.1 Overview of polymer synthesis

The mechanism that is used to join a series of monomers into a polymer will depend upon the functionality that the monomers display; in turn, the properties of a polymer may vary according to the method by which it was synthesized. Some common polymerization methods include free radical polymerization, controlled radical polymerization, and condensation (step-growth) polymerization, and each of these mechanisms can employ the same constituent monomers to produce polymers with

different characteristics (provided that the monomers have the appropriate functionality). In addition, within these broad categories there often exist a number of sub-types of polymerization reactions, further diversifying the synthesis options that are available to the polymer chemist.

The variability of outcome that exists between the above polymerization methods derives from the different methods by which they proceed and the associated differences in reaction kinetics. For example step-growth polymerization occurs, as the name suggests, via stepwise reactions between the functional groups on reactants with two or more complementary functional groups. This type of polymerization does not proceed from any particular "active center"; rather, monomers react essentially at random in solution, forming larger and larger oligomers until conversion approaches 100% and oligomers can react to form high-MW polymers. As a consequence, forming high-MW polymers via step-growth polymerization is often difficult and requires longer reaction times, but those polymers retain their functionality at their end-groups (i.e. further polymerization can proceed following the addition of the appropriate monomer) [52]. On the other hand, free radical polymerization proceeds from an active radical site that adds monomers (most often containing unsaturated carbon-carbon bonds) to a growing chain one at a time, until two active sites meet and react to quench both their radicals. In this case, a high-MW is achieved very early on in a reaction; however, once all of the radicals have been consumed, it is no longer possible to extend the polymer chains (note that there are exceptions for certain derivatives of this type of reaction; these will be discussed below) [52]. The examples above only serve to highlight some of

the differences between these types of polymerization reactions; a brief summary of some other defining characteristics is given in Table 2 – 1.

Table 2 - 1. Differences between types of polymerization reactions.

Type	Relevant monomer	Polymer	Pros	Cons
Free-radical	Ethylene 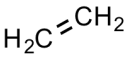	Polyethylene 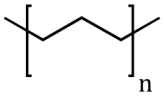	- usually high conversion; relatively fast	- poor control; final product will be mixture of various sized polymers
Controlled radical (CRP)	Ethylene 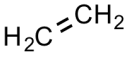	Polyethylene 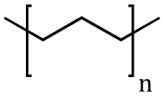	- able to achieve controlled, living polymerization with a wide variety of monomers	- some types of CRP use toxic metal catalysts; conversion can be poor
Step-growth	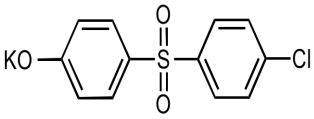	Polyethersulfone 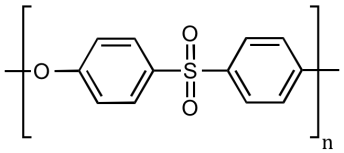	- poly-merization is living	- long reaction times are required to achieve high MW

2.2.2 Reversible Addition-fragmentation chain Transfer (RAFT)

The free radical method of polymerization described above has the advantage of being able to quickly produce large polymers at high rates of conversion. However, the random nature of the termination and/or disproportionation events that terminate this type of reaction results in a product consisting of a large distribution of polymer sizes around some mean. The high polydispersity index (PDI) of these polymers presents a

problem for reproducibility between batches that, in addition to producing inconsistent properties, may also be a hurdle to achieving regulatory approval of new biomaterials. Furthermore, once all of the radicals in a free-radical polymerization have been consumed, it is no longer possible to extend polymer chains produced in this manner unless some sort of orthogonal functional group was included in the primary chain. This makes it difficult to produce block copolymers, and other, similar systems which seek to combine the properties of two or more types of polymers. The need exists, therefore, for a method of polymer synthesis that can produce polymers in a controlled fashion while still instilling a "living" character (i.e. the ability for further extension of polymer chains beyond the initial polymerization reactions)

Some condensation polymerizations can proceed in a controlled manner [53], but in the realm of radical polymerization two primary methods have been developed to achieve this goal. Atom-transfer radical polymerization (ATRP) controls dispersity via an equilibrium between a propagating radical and a dormant species (commonly an alkyl halide – macromolecular species); exchange between the two is mediated by the inclusion of transition metal complexes [54]. Due to the potential toxicity and challenges with removal of these complexes in the context of biomedical applications, this method was not used to produce the polymers in this study and will not be further discussed. The other commonly used method for achieving control over radical polymerizations is known as reversible addition-fragmentation chain transfer (RAFT). In this scheme, polymerization reactions can often be prepared in much the same way as the might be for a conventional free radical polymerization, save for the inclusion of a specific

molecule known as a RAFT agent. The RAFT agent (Fig. 2 – 4) is a chain transfer agent with a high transfer coefficient (most commonly structured around a thiocarbonylthio group) which is able to confer a living character to radical polymerizations transferring a radical between two growing chains, such that the chains are not able to terminate prematurely [55]. The mechanism of a RAFT reaction includes the following five steps (Fig. 2 – 5) [55]:

Initiation: An initiator generates a radical species (i.e. via thermal decomposition), which attacks the vinyl group of a monomer producing an active polymer chain (P_n•).

Initial Equilibrium: P_n• quickly reacts with the C=S group of the RAFT agent to form an intermediate adduct radical; this will undergo reversible fragmentation towards either the initial chain, or towards the R-group of the RAFT agent.

Re-initiation: The leaving R-group of the RAFT agent produces a radical (R•) that goes on to initiate a new active polymer chain (P_m•).

Main equilibrium: The new active chain (P_m•) either continues to grow or binds to the RAFT agent-P_n• complex. In the latter case, fragmentation subsequently occurs and either P_n• or P_m• is de-coupled from the RAFT agent, whereupon the de-coupled chain can continue to grow while the other chain is sequestered in a dormant state in the polymer-RAFT agent complex. In this way, the potential for an encounter between two growing radical chains is minimized, and so too is the potential for random termination.

Termination: Although RAFT is designed to limit termination, it is still possible for two or more growing chains to encounter one another and consume their radicals. However, with proper selection of RAFT agents and appropriate experimental conditions, this step should be minimized and should not significantly affect the dispersity of the final product.

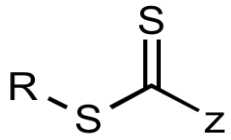

Figure 2 - 4. Generic structure of a dithioester-based RAFT agent. Z is a stabilizing gorup, while R represents the leaving group.

The RAFT reaction was first reported in the late 1990's by the research group of Dr. Graeme Moad at the Commonwealth Scientific and Industrial Research Organization (CSIRO) in Australia [56]. Since then the simplicity of the RAFT reaction and its compatibility with a wide variety of monomers have led to its adoption as one of the methods of choice for achieving controlled and living polymerizations [57]. In addition to improving the reproducibility of polymerization reactions, RAFT has also been used to mediate certain types of polymerization that would be unsuccessful were they to be conducted in an uncontrolled manner. For example, Luzon and colleagues used RAFT techniques to produce hyperbranched polymers of OEGMA and $M(EO)_2MA$. Without the presence of the RAFT agent, this type of polymerization will often result in the formation of gels due to the uncontrolled nature of the reaction [58].

i Initiation

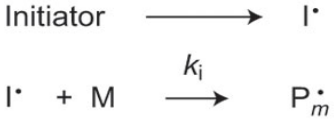

ii Initial equilibrium

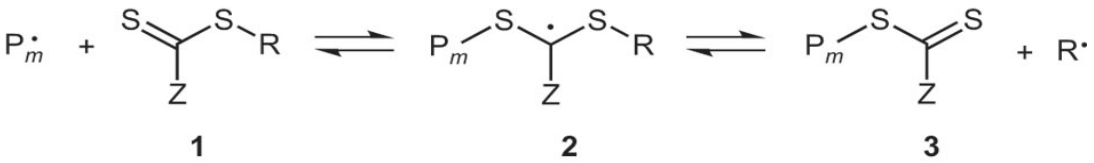

iii Reinitiation

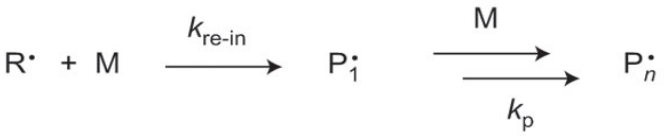

iv Main equilibrium

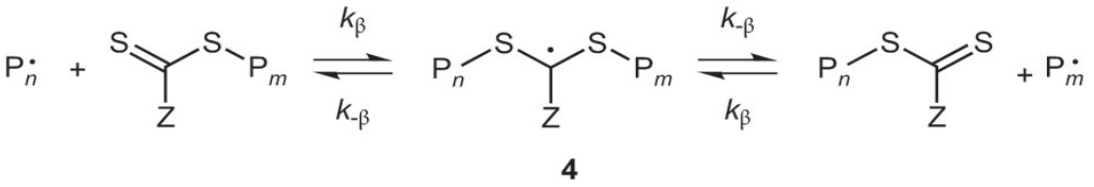

v Termination

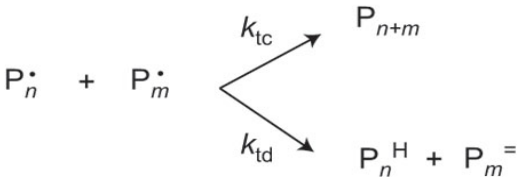

Figure 2 - 5. Mechanism of a RAFT reaction**.** *Figure adapted from the literature [59].*

Another area in which RAFT technology has been extensively applied is the production of block copolymers. The living nature of the RAFT reaction makes it easy to extend polymer chains, often by simply adding additional monomer and heating the reaction. The efficiency of this process has allowed the production of a variety of complex copolymers containing multiple blocks capable of forming systems that can exhibit a wide range of properties (as determined by their constituent chains). Some examples include block copolymer-based nano-objects produced via RAFT aqueous dispersion polymerization [60], block copolymer based amphiphilic brushes for the stabilization of colloidal drug delivery systems [61], and pseudo-zwitterionic block copolymer coatings for medical devices with anti-fouling properties [62].

This study used RAFT techniques extensively to produce a variety of well-defined POEGMA polymers with different sizes and architectures. These polymers were used to explore what effects precursor structure would have on the biomaterial properties of injectable hydrogels. More details on the specific RAFT reactions used in this study are given in the proceeding chapters.

2.2.3 Precursor molecular weight effects on the properties of hydrogels

As has been mentioned throughout this review, one of the major benefits of using hydrogels as biomaterials is the potential for high tunability that they offer. By changing such factors as precursor monomer composition, post-polymerization functionalization, or peptide distribution, a variety of hydrogels can be made that exhibit a range of physical and chemical properties. While many methods for modulating hydrogel properties involve changing the chemical structure of polymeric

precursors (i.e. changing functional group density in order to change cross-link density in covalently bonding polymers), other modulation targets are also being explored. One such target is the MW of the precursor polymers themselves. The MW of a polymer can have a wide range of effects on that polymer's physical characteristics. These include properties such as the LCST [63], viscosity [64], and rates of uptake by cells [65], among many others. Additionally, when using polymers in an *in vivo* context, it is important that the size of the polymer (the size being related to MW) not exceed the renal clearance limit (approx. 5 – 6 nm for globular proteins) so that they can be efficiently removed from the body once they have served their function [66]. Given the effect that polymer MW has on the properties of the polymers themselves, it is unsurprising that polymer MW would also affect hydrogel properties when polymers are cross-linked to form a gel. Changing the MW of precursor polymers has been shown to affect properties such as hydrogel swelling, mechanical strength, and elasticity, amongst many others [67]. The variation in these properties can go on to affect how these gels perform as drug delivery systems or tissue engineering scaffolds. In the former case, the change in mesh size or degradation rates that can be associated with a change in precursor MW can affect the loading capacity of a hydrogel, and the rate of drug release from that gel [68]. In the latter case, by affecting properties such as mechanical strength, changing the MW of polymers could potentially dictate how cells behave when they are seeded on or in a hydrogel construct. In fact, one of the principle draws of modulating hydrogel properties in this manner is the potential to alter their physical characteristics (i.e. mechanical strength), while maintaining a more or less uniform chemical environment.

In vivo, cells respond to a variety of factors in their immediate surroundings, including the elasticity of the local ECM, the presence of certain signaling molecules, and the density of cell distribution [69]. In tissue engineering in general, and in the context of hydrogels in particular, changing properties such as mechanical strength often involves a chemical change in the matrix as well (i.e. increasing functional group density), which can make it difficult to determine how exactly certain matrix factors are affecting the growth and behavior of cells that are distributed within these tissue engineering constructs. Using the MW of precursors to control the properties of these constructs offers the opportunity for precise tuning of hydrogels, further expanding their potential as a biomaterial. This work investigates the effect of precursor MW on the properties of injectable POEGMA hydrogels. Experiments were performed to determine how precursor MW affects the swelling, degradation, mechanical properties etc. of these POEGMA gels. The potential for these POEGMA polymers to support cellular growth was also assessed.

2.2.3 Hyperbranched polymers

Thus far, this review has covered a number of variable chemical and structural factors of polymers (and monomers) that can be altered to produce biomaterials with a range of properties. Another feature of polymers that can be exploited to produce new kinds of materials is the architecture of the polymers themselves. Extensive research has already been focused on producing non-linear polymers, and the result has been the development of polymers with a variety of geometric structures such as star polymers, brush polymers, ladder polymers, *etc.* [55]. One type of molecular architecture that has

attracted particular attention is the so-called "branched" polymer structure. Branched polymers exist in two major categories: dendrimers, which have almost perfect radially-symmetric branching (degree of Branching (DB) = 1), and hyperbranched polymers, which have a DB somewhere between 1 and 0 (Fig. 2 – 6) [70]. Dendrimers are most commonly formed via a multistep polymerization that begins with a single multifunctional molecular core and then proceeds outwards in subsequent generations to produce a collection of globular, and almost perfectly monodisperse, macromolecules [71]. Ultimately, in addition to being well defined, these molecules display a number of properties that make them attractive as artificial biomaterials, including a high degree of functional versatility (due to a potentially large amount of chain-end functional groups), compact macromolecular structure, and high solubility [72]. Researchers have exploited these properties to produce nanoparticles for anticancer drug delivery [73], contrast agents for magnetic resonance imaging [74], and a variety of other clinically relevant biomacromolecules [72]. However, one of the major issues with the broad-scale application of dendrimers is the often-laborious nature of their synthesis; multiple activation, deactivation, and purification steps are often needed to maintain their characteristic uniformity of branching. Alternatives have arisen, therefore, in the form of hyperbranched polymers, irregularly shaped polymers with a degree of branching that lies somewhere between the DB of linear polymers and dendrimers [75]. The major advantage of these types of polymers is that they can be produced by relatively straightforward, often one-pot synthesis methods while still retaining much of the functional versatility and structural compactness of dendrimers [76].

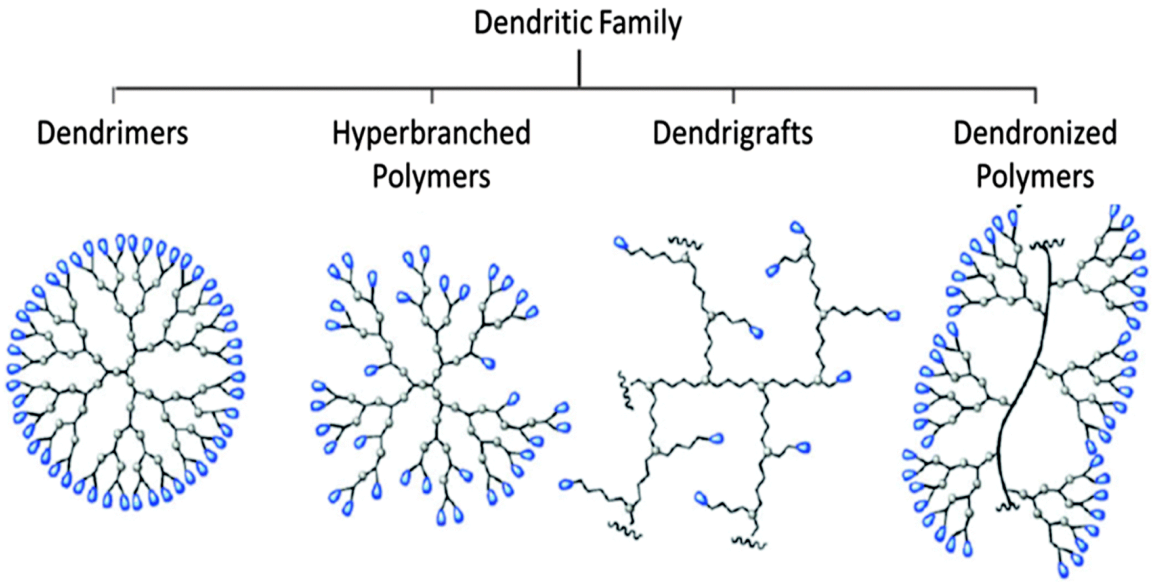

Figure 2 - 6. Types of dendritic polymers. The terminal blue points indicate terminal functional groups for possible chain extension. *Figure adapted from the literature [77]*.

The relative simplicity of hyperbranched polymer synthesis also means that these polymers are better candidates for the eventual scale-up of biomacromolecule production that would be needed if any of these molecules were to be applied clinically. Indeed, researchers have suggested substituting hyperbranched molecules in many of the applications for which dendrimers had previously shown particular promise. For example, in 2012 Liu and colleagues described a self-assembling diseleinide-containing amphiphilic hyperbranched phosphate that was able to form nanomicelles in water that can inhibit the proliferation of cancer cells [78]. Another example comes from Asri and colleagues, who used hyperbranched polyurea as a base onto which they could anchor quaternary ammonium compounds to produce a coating which had antibacterial and antifouling properties [79].

This study explores the use of hyperbranched polymers as hydrogel precursors. Controlled radical polymerization (CRP) techniques are used to produce functional

hyperbranched POEGMA polymers with varying degrees of branching. These polymers are subsequently used to form injectable hybrid hydrogels composed of linear/hyperbranched POEGMA polymers.

3 Tuning the Properties of Injectable POEGMA Hydrogels by Controlling Precursor Polymer Molecular Weight

3.1 Introduction

Relative to natural polymers, one of the principle advantages of using hydrogels based on synthetic polymers for biomedical applications is the high tunability of the precursor materials. By controlling such factors as which monomers are used to prepare the polymer(s), the reaction conditions of the polymerization, and which method is used to polymerize the monomers, synthetic polymers can be tailored to exhibit properties that make them suitable for use in a wide variety of clinical and laboratory applications [80]. Furthermore, synthetic polymers typically offer greater opportunities for post-polymerization functionalization than their natural counterparts, expanding the potential for designing materials with highly tailored mechanical strengths, degradation rates, hydrophobicities/hydrophilicities, and cellular interactions, among other key properties [81].

One group of synthetic polymers that has attracted widespread research interest is poly(ethylene glycol) (PEG) and related polymers. These polymers have a number of properties that make them potentially useful for drug delivery and tissue engineering applications, including their high hydrophilicity, anti-fouling properties, and general non-cytotoxicity [82]. However, the chain end-only functionality of PEG inherently limits its synthetic versatility, particularly in the case of PEG-based hydrogels in which these end functional groups are also required for effective crosslinking. This limitation has led to interest in the development of PEG-analogue polymers that have similarly desirable

biological properties but also offer more opportunities for functionalization. One particularly well-studied analogue is poly(oligoethylene glycol methacrylate) (POEGMA), which consists of PEG side-chains off a methacrylate backbone [44]. The methacrylate group on the OEGMA monomer facilitates its polymerization via (controlled) radical polymerization, enabling the use of a variety of copolymerization strategies to functionalize the polymers as desired. An early example of the applications of POEGMA comes from Haddleton and co-workers in 2004. This group polymerized OEGMA using controlled radical polymerization using its increased functionality to introduce terminal aldehydes into the polymers. The residual aldehyde group allowed them to conjugate their polymers to proteins through the formation of a Schiff base. Proteins that were attached to the polymers in this way would be hidden from the body's immune response, allowing for their potential oral administration in certain protein-based therapies [83]. More recently, the Battaglia group used POEGMA in the hydrophilic portion of an amphiphilic block co-polymer for the facilitation of mesenchymal progenitor cell adhesion. The team functionalized the POEGMA portion of the polymers with RGD for cell adhesion, while the hydrophobic portion of the polymer remained cell-inert; this produced a molecule that mimicked the segmented adhesive properties of the extracellular matrix (ECM). The group went on to show that mesenchymal progenitor cells preferentially adhered to the mixed cell-adhesive/cell-inert polymer, when compared to entirely cell-adhesive, or entirely cell-inert molecules [84]. A selection of other examples of POEGMA use from the literature can be found in the references section [85-87].

Recently, our group has published extensively on the development of *in situ* gelling hydrogels based on POEGMA precursor polymers functionalized with complementary hydrazide/aldehyde functional groups [50, 51, 88-91]. We have demonstrated effective modulation of properties such as the mechanical strength and degradation rates of these gels by changing the degree of functionality of the precursor POEGMA polymers and the length of the PEG side chains of the constituent monomers. Furthermore, we have applied this chemistry to create bulk hydrogels, thin hydrogel films on porous substrates (e.g. paper), and fibrous hydrogel networks formulated via electrospinning. In each case, the molecular weight of the precursor polymers was controlled by simple chain transfer polymerization, leading to the generation of polymers with somewhat broad polydispersities (1.6 – 2.5) but molecular weights consistently below the renal filtration limit to promote clearance of the polymers following the degradation of the hydrazone crosslinked gel networks [88]. However, while controlling the molecular weight of natural polymers has been explored as an avenue to control gel properties [68, 92], there are to our knowledge no reports of how controlling the molecular weight of synthetic precursor polymers to *in situ*-forming hydrogels can be used to manipulate properties. This approach holds particular appeal given that, unlike increasing the mole fraction of crosslinking groups or changing the monomer mixture along the polymer backbone, changes in the molecular weight and thus the gel properties can be achieved without significantly altering the chemistry of the precursor polymers. As such, manipulation of hydrogel properties by controlling molecular weight has potential to facilitate more predictable changes in gel

performance in applications such as drug delivery (i.e. only diffusion and not partitioning is altered) or tissue engineering (i.e. only mechanics but not protein adsorption is altered). In particular, such control could be useful for isolating the effects of certain substrate properties (such as mechanical strength) on the behavior of cells that are grown on that substrate while controlling for the confounding variables of changing chemistry [93-96]. Furthermore, by using controlled free radical polymerization techniques such as reversible addition-fragmentation chain transfer (RAFT), well-defined precursor polymers can be produced with improved reproducibility and greater batch-to-batch uniformity [57, 97, 98], both of which have potential benefits in creating more consistent hydrogel properties and increasing the likelihood of regulatory approval [99].

Herein, we demonstrate the use of RAFT to create well-defined POEGMA precursor polymers of four distinct molecular weights (all below the renal clearance limit) but the same monomer and reactive functional group contents. The properties of these polymers, and the hydrogels they produced, were investigated to show how the molecular weight of *in situ*-gelling precursor polymers can be manipulated to control the swelling, degradation, mechanics, and interfacial biological properties of POEGMA hydrogels without significantly altering the chemistry of the precursor polymers. We anticipate that the insight derived will have significant applications in the rational development of POEGMA-based hydrogels that have properties that are engineered for various drug delivery and tissue engineering applications.

3.2 Materials & Methods

3.2.1 Materials

All chemicals were purchased from Sigma Aldrich (Oakville, ON) unless otherwise noted. Di(ethylene glycol) methyl ether methacrylate ($M(EO)_2MA$, 95%), oligo(ethylene glycol) methyl ether methacrylate ($OEGMA_{475,}$ 95%) with an average molecular weight of 475 g mol^{-1}, and methacrylic acid (MAA, 99%) were purified via passage over a column of basic aluminum oxide (type CG-20) to remove the methyl ether hydroquinone (MEHQ) and butylated hydroxytoluene (BHT) inhibitors. Azobisisobutyronitrile (AIBN, 95%), 2-cyano-2-propyl 4-cyanobenzodithioate (CPCDB, 98%), adipic acid dihydrazide (ADH, Alfa Aesar, 98%), N'-ethyl-N-(3-dimethylaminopropyl)-carbodiimide (EDC, Carbosynth, Compton CA, commercial grade), aminoacetaldehyde dimethyl acetal (ADA, 99%), and N-hydroxysuccinimide (NHS, 98%) were used as received. 3T3 *Mus musculus* mouse cells were obtained from ATCC: Cedarlane Laboratories (Burlington, ON). Dulbecco's modified Eagle medium (+glucose, +pyruvate, DMEM), fetal bovine serum (FBS), penicillin/streptomycin (PS), and trypsin-ethylenediaminetetraacetic acid were purchased from Invitrogen Canada (Burlington, ON). 1,4-Dioxane (reagent grade), dichloromethane (DCM, reagent grade), and diethyl ether (reagent grade) were purchased from Caledon Laboratory Chemicals (Georgetown, ON). Hydrochloric acid (HCl, 1M) was received from LabChem Inc. (Pittsburgh, PA). Milli-Q grade distilled deionized water (DIW) was used for all experiments.

3.2.2 Polymer synthesis

3.2.2.1 Controlled synthesis of poly(oligoethylene glycol methyl ether methacrylate-co-methacrylic acid (POEGMA-co-MAA)

In a typical experiment (Table 3 – 1, entry $PO_{15.9}$) the polymer was prepared by adding AIBN (9.26 mg, 0.0564 mmol), CPCDB (49.65 mg, 0.2 mmol), $M(EO)_2MA$ (4.0 g, 21.2 mmol), $OEGMA_{475}$ (1.12 g, 2.36 mmol), and MAA (0.872 g, 10.13 mmol) to a 100 ml Schlenk Flask. Dioxane (20 ml) was added to the reaction mixture, the reaction vessel was sealed, and the solution was purged via three freeze-pump-thaw cycles. The flask was then backfilled with nitrogen and subsequently submerged in a preheated oil bath at 70 °C for 24h under magnetic stirring. After 24h, the reaction vessel was removed from the oil bath and the reaction was terminated by rapid cooling in an ice bath and exposure to oxygen. A sample of the crude reaction mixture was taken for NMR analysis, and the remainder of the solution was purified via precipitation in 10x cold ethyl ether. The resulting precipitate was dried under vacuum for 4+ hours and used for compositional analysis. A series of four polymers was prepared with a range of targeted molecular weights (10,000 – 30,000 g/mol, with the upper limit of 30,000 chosen based on the renal filtration limit) [100], with the recipes of each polymer prepared shown in Table 3 – 1. The $PO_{6.7}$ – $PO_{15.9}$ polymers, where the subscript represents the M_n as measured by GPC, used the same total number of moles and ratios of monomers (33.7 mmol total monomer; $M(EO)_2MA/OEGMA_{475}$/MAA = 63/7/30) but varying numbers of moles of the CPCDB RAFT agent to change the targeted number average molecular weights of these polymers, as per Eq. 3 – 1 .

$M_{n,theory} = M_{avg} \times [m]/[c]$ Eq. 3 – 1

Here, M_{avg} is the average MW of monomers and [m] and [c] are the concentrations of monomer and RAFT agent respectively.

3.2.2.2 Synthesis of hydrazide-functionalized POEGMA-co-MAA (POH_n)

In a typical experiment ($POH_{15.9}$), precipitated POEGMA-co-MAA was dissolved in 100 ml of DIW. ADH (8.82 g, 10 mol excess) was added to this solution, and the pH of the mixture was dropped to 4.75 via the addition of 1 M HCl. Subsequently, EDC (2.75 g, 3.5 mol excess) was added to the reaction, and the pH of the solution was maintained at 4.75 by addition of 1 M HCl for 5+ hours. Once the pH of the solution was stable, the reaction was left to stir overnight. The solution was then transferred to regenerated cellulose dialysis tubing (MWCO = 3.5 kDa) and dialyzed against 5 L of DIW for 6 cycles of at least 6 hours each. The polymer solution was subsequently lyophilized to dryness, yielding a white powder that was stored at 4 °C prior to use.

3.2.2.3 Synthesis of aldehyde-functionalized POEGMA-co-MAA ($POA_{15.0}$)

POEGMA-co-MAA with controlled molecular weight ($M_{n,theory}$ = 30000 Da) was prepared according to the method described in section 3.2.2.1. The resulting precipitate was dissolved in 50 ml of DCM, to which was added NHS (2.33 g, 2 mol excess) and EDC (3.15 g, 2 mol excess). The solution was allowed to react under magnetic stirring for 6 h at room temperature. Subsequently, ADA (3.19 g, 3 mol excess) was added to the solution and stirred overnight at room temperature to graft acetal groups to the

polymer backbone. The polymer was then precipitated out of solution in 10x cold ethyl ether, and the precipitate was re-dissolved in 150 ml of DIW. Once the polymer had completely dissolved, 25 ml of 1 M HCl was added to the solution, and the reaction was allowed to stir overnight at room temperature to cleave the acetal groups to aldehydes. The reaction was subsequently transferred to 3.5 kDa MWCO regenerated cellulose dialysis tubing and dialyzed against 5 L of DIW for 6 cycles of at least 6 h each. The solution was then lyophilized to dryness to yield the product (a white powder) that was stored at -20 °C prior to use.

Table 3 - 1. Synthesis recipes for well-defined unfunctionalized POEGMA polymers**.**

Polymer	Monomer/CPCDB	Monomer/AIBN	$M_{n,\ theory}$
$PO_{6.7}$	56/1	197/1	10,000
$PO_{9.3}$	84/1	295/1	15,000
$PO_{11.6}$	113/1	394/1	20,000
$PO_{15.9}$	169/1	592/1	30,000
$PO_{15.0}$	169/1	592/1	30,000

3.2.3 Characterization of functionalized POEGMA polymers

The degree of polymer functionalization was determined via conductometric titration on a 50 mg sample of each polymer in 50 ml of 1 mmol NaCl solution, using 0.1 M NaOH as the titrant. The results of these titrations were compared against the titration result from the corresponding unfunctionalized sample in order to determine the efficiency of the functionalization reactions. Titrations were repeated in triplicate, and reported functional group content results represent the average of those values.

Aqueous size exclusion chromatography (SEC) was performed using a system consisting of a Waters 515 HPLC Pump, a Waters 717 Plus autosampler, three ultrahydrogel columns (30 cm x 7.8 mm i.d.; 0 – 3 kDa, 0 – 50 kDa, 2 – 300 kDa), and a Waters 2414 refractive index detector. A mobile phase consisting of 0.5 M $NaNO_3$, 25 mM CHES buffer (pH 10.4), and 10 ppm NaN_3 was used for all polymers (flow rate = 0.8 ml min^{-1}). The elution time of the polymers was compared against linear PEG standards ranging from 106 to 584 **kDa** (Waters).

^{1}H-NMR analysis of the polymers was performed at various stages during the synthesis process using a 600 MHz Bruker AVANCE spectrometer and deuterated DMSO as the solvent. The percent conversion achieved during the reactions was determined by taking a ^{1}H-NMR sample of the crude reaction mixture immediately following the reaction and comparing the signal from the vinyl protons against the signal from the polymer backbone according to Eq. 3 – 2 (C**H$_2$**=CH-, δ = 5.6 – 6; -C**H**$_2$-, δ = 1.6 – 2):

$$\text{Conv.} = \tfrac{1}{2}I_{1.6\text{-}2}/(\tfrac{1}{2}I_{1.6\text{-}2} + I_{5.6\text{-}6}) \qquad \text{Eq. 3 -2}$$

The mole fraction of $M(EO)_2MA$ to $OEGMA_{475}$ incorporated into the polymer was determined according to the method described previously by Wang et al. [36].

The cloud point of each polymer, related to its LCST, was determined using a Variant Cary Bio 100 UV-vis spectrophotometer. The polymers were dissolved to a concentration of 5 mg ml^{-1} in 10 mM PBS (pH = 7.4); measurements were then taken

over a temperature ramp from 10 to 80 °C at 0.5 °C intervals, with the temperature raised at a rate of 1 °C min^{-1}.

3.2.4 Preparation of *in situ* gelling hydrogels

Solutions of the functionalized POEGMA polymers were prepared by dissolving the dry polymer in 10 mM PBS (pH = 7.4) to a concentration of 15% w/v. The different POEGMA hydrogels were prepared by pipetting equal proportions of one of the POH_n polymers with the $POA_{15.0}$ polymer into cylindrical silicone rubber molds. The dimensions of the molds varied according to the test that was to be performed on the gels: for swelling/degradation, diameter = 9 mm, volume = 240 µl; for rheology, diameter = 11.5 mm, volume = 500 µl. Following deposition into the mold, the polymers were mixed manually by vigorous repeated pipetting with a 1 ml pipette for 5 – 10 seconds, and subsequently allowed to gel overnight in a sealed container (with 100% relative humidity) at room temperature prior to testing. Gelation time of the POEGMA gels was assessed by extrusion of 50 µl each of the 15% w/v functionalized precursors into a sealed test tube (volume = 2 ml) and subsequent manual rotation of the tube every 5 s; the gelation time was defined as the time point at which the gel was no longer visibly seen to flow (after 10 seconds of observation time).

The quantity of residual hydrazide and aldehyde functional groups remaining after gelation in each of the POEGMA gels was assessed using a fluorescein fluorescence assay. Polymer solutions were diluted to a working concentration of 150 mg ml^{-1} in 10 mM PBS, and gels were subsequently prepared by mixing 30 µl of one of the POH_n polymer solutions with 30 µl of the $POA_{15.0}$ polymer solution in the wells of a 48-well

tissue culture plate. Solutions of 0.05 g L^{-1} 5-FTSC (aldehyde reactive) or 0.05 g L^{-1} 5-FITC (hydrazide reactive) were prepared in carbonate buffer (pH = 8.5). After the gels had been allowed to equilibrate overnight at room temperature, 150 µl of the 5-FTSC solution was added to each well. The gels were allowed to soak in the solution overnight, after which time non-reacted probe was removed from the gels via 15 x 5 minute wash cycles in fresh carbonate buffer. This process was repeated using another set of plates for the 5-FITC solution. After washing, the fluorescence of each plate was read using a Biorad plate reader (model 550; λ_{exc} = 488 nm, λ_{emi} = 535 nm). Results are reported as the mean of three replicate measurements, and error bars represent one standard deviation from the mean.

3.2.5 POEGMA hydrogel transparency

The transmittances of the POEGMA gels were assessed at 595 and 405 nm wavelengths. Gels were prepared by mixing equal volumes (30 µl each) of one the POH_n polymers and the $POA_{15.0}$ polymer in the wells of a 96-well polystyrene tissue culture plate. The plates were sealed to prevent the gels from drying out, and the gels were allowed to equilibrate overnight. The absorbance of each gel was subsequently measured at the aforementioned wavelengths using a Biorad multi-plate reader. The readings from the gels were normalized against the readings from wells containing an equal volume of 10 mM PBS. Absorbances were converted to transmittance values according to Eq. 3 – 3:

$$A = 2 - \log(T) \qquad \text{Eq. 3 – 3}$$

Results are reported as the mean of replicate measurements, and error bars represent one standard deviation from the mean (n = 3).

3.2.6 Swelling and degradation kinetics

The swelling kinetics of the POEGMA gels were assessed in 10 mM PBS at 22 °C. The gels (with weight W_0) were removed from the silicone rubber molds and transferred into pre-weighed cell culture inserts, which were subsequently placed into 12-well cell culture plates containing pre-warmed 10 mM PBS (4 ml/well). At predetermined time intervals, the inserts plus gels were removed from the PBS, the PBS was drained from the inserts, and when necessary excess PBS was wicked off from the surface of the gels using a Kimwipe prior to weighing (W_t). The hydrogels were then re-submerged in 4 ml of fresh pre-warmed PBS, and the measurements were continued until all the gels had reached equilibrium swelling ratios and then subsequently degraded (approx. 4 days, determined visually). The swelling ratio (SR; equivalent to normalized hydrogel weight) of the gels at any given time point (m_t) was determined according to Eq. 3 – 4:

$$SR = W_t/W_0 \qquad \text{Eq. 3 – 4}$$

Swelling of the POEGMA gels was modeled over the first 10 hours of swelling using a first-order kinetics expression of the form $(W_t/W_0)_t = (W_t/W_0)_{max}\ (1 - e^{-kt})$ allowing for fitting of the swelling rate constant *k*.

The degradation kinetics of the POEGMA gels were assessed in 10 mM PBS and 10 mM HCl respectively at 37 °C, with the HCl test representing an accelerated degradation experiment facilitating more direct comparisons between the hydrolytic stability of different gels on a shorter timescale. Degradation was tracked gravimetrically using the same method used for swelling kinetics, with measurements repeated until the gels could no longer be visually distinguished as a separate phase.

All experiments were repeated in triplicate, and reported results represent the average of these measurements. Error bars represent one standard deviation from the mean.

3.2.7 POEGMA hydrogel rheology

The rheological properties of the POEGMA gels were characterized using a Mach-1 Mechanical Tester (Biomomentum Inc., Laval, QC) operating under parallel plate geometry at room temperature. POEGMA hydrogel disks (diameter = 11.5 mm, height = 3.5 mm) that had been allowed to gel overnight were transferred from the silicone mold to the mechanical tester. The compressive modulus of the gels was determined by compressing the gels to 75% of the original sample height at a rate of 3% s^{-1}. Shear testing was performed by pre-compressing the gels to 75% of the sample height and subsequently subjecting them to a strain sweep test using amplitudes ranging from 0.1 to 2.2° at 0.5 Hz to determine the linear viscoelastic region (LVE) of the gels. The gels were subsequently subjected to a dynamic frequency sweep (0.1 to 2.2 Hz) within the LVE to determine their shear storage modulus (G'). All experiments were repeated in

triplicate; reported results represent the average of these replicates, with error bars representing one standard deviation from the mean.

3.2.8 *In vitro* POEGMA cytotoxicity assay

The cytotoxicity of POEGMA polymers was assessed using the resazurin cytotoxicity assay [101]. Briefly, 3T3 mouse fibroblasts were plated at a density of 10,000 cells/well in a 96-well polystyrene tissue culture plate and incubated for 24 h at 37 °C in DMEM supplemented with FBS (10%) and penicillin/streptomycin (1%). Cells in the experimental wells were subsequently exposed to solutions (prepared in DMEM and sterilized via passage through a 0.2 μm Acrodisc filter (Pall) prior to testing) of each of the polymers at concentrations ranging from 200 to 2000 μg ml^{-1}. The cells were incubated with the polymers for 24 h at 37 °C, followed by addition of resazurin sodium salt solution (in PBS) such that the final concentration of resazurin in each well was 10 μg ml^{-1}. The cells were subsequently returned to the 37 °C incubator for 4h. The fluorescence of each of the wells was then measured using a Biorad plate reader (model 550; λ_{exc} = 531 nm, λ_{emi} = 572 nm). Background fluorescence was accounted for by subtracting the fluorescence reading of blank wells (n = 2) from the readings of the corresponding experimental wells. The fluorescence readings from the experimental wells were compared against the readings from untreated (cell-only) controls to determine relative cell viability. Error bars represent the standard deviations of the measured cell viability percentages (n = 4).

3.2.9 Statistical analysis

Statistically significant differences between any pair of samples were determined using a two-tailed t-test with $p < 0.05$ assuming unequal variances.

3.3 Results & Discussion

3.3.1 Characterization of well-defined functional POEGMA polymers

Well-defined POEGMA polymers with complementary hydrazide/aldehyde functionalities were synthesized via controlled RAFT polymerization (Fig. 3 – 1). A series of four different hydrazide polymers ($POH_{6.7}$ – $POH_{15.9}$) and one aldehyde polymer ($POA_{15.0}$) were prepared with targeted number average molecular weights ranging from 10,000 to 30, 000 Da. Aqueous GPC analysis of the final polymer products shows that each polymer in the series had a measured M_n below its targeted (theoretical) molecular weight based on the recipe used (Table 3 – 2), a result we attribute to the calibration of the GPC with linear PEG standards. Previous work has shown that star and comb polymers regularly deviate from expected M_n values when assessed by a GPC calibrated with linear standards given that the more compact comb polymer architecture produces molecules with smaller hydrodynamic radii at a given molecular weight [102]. However, each polymer's M_n accurately reflected its position in the series (i.e. $PO_{9.3}$ is larger than $PO_{6.7}$), such that a series of well-defined precursor polymers with different molecular weights was successfully synthesized. All polymerizations proceeded to a high conversion (> 85%) over the 24h time period of the reaction. Furthermore, the dispersity of all of the polymers in the series was low (Đ < 1.3), indicating that

polymerization proceeded in a controlled manner (Table 3 – 2). Note also that other papers have reported similarly high conversions and low dispersities when using this CPCDB RAFT system for OEGMA polymerization [103]. The small differences in PDI that were observed between the polymers in the series are likely due to differences in the size of the ethylene glycol side chain among the $OEGMA_{475}$ monomers that were used in the reactions. While POEGMA polymers can exhibit a cloud point in solution, the 90:10 $M(EO)_2MA$:$OEGMA_{475}$ mole ratio used resulted in high and (as expected given their chemical similarity) consistent cloud point values well above both room and physiological temperature; the cloud points of the $POH_{6.7}$ – $POH_{15.9}$ polymers ranged from 76 – 79 °C while the cloud point of the aldehyde functionalized $POA_{15.0}$ was 64 °C, with the lower cloud point of the aldehyde polymer consistent with the lower hydrophilicity of the aldehyde relative to the hydrazide reactive functional group (Table 3 – 3; Appendix Fig. A – 1) [90]. Titration prior to hydrazide/aldehyde functionalization showed nearly stoichiometric incorporation of the functional monomer (MAA) in all of the $PO_{6.7}$ – $PO_{15.9}$ polymers as well as $PO_{15.0}$ (Table 3 – 2). $M(EO)_2MA$ and $OEGMA_{475}$ were similarly incorporated at approximately uniform ratios across the full series of precursor polymers prepared (mol% $M(EO)_2MA \approx 70$, mol% $OEGMA_{475} \approx 4$; Table 3 - 2). However, relative to the recipes, $M(EO)_2MA$ was somewhat preferentially incorporated into the polymers, a result we attribute either to a lower $k_{dissociation}$ for $OEGMA_{475}$ in regards to its proclivity to dissociate from the RAFT agent or steric issues with the incorporation of the long ethylene glycol side chain of $OEGMA_{475}$ into the polymer [48].

Table 3 - 2. Characterization of unfunctionalized POEGMA polymers.

Polymer	$M_{n,theory}$ (kDa)	M_n (kDa)	M_w (kDa)	Đ	MEO_2MA (mol %)	$OEGMA_{475}$ (mol %)	MAA (mol %)	Conv.
$PO_{6.7}$	10	6.7	8.5	1.25	70	4	26	0.97
$PO_{9.3}$	15	9.3	11.0	1.19	69	4	27	0.97
$PO_{11.6}$	20	11.6	13.9	1.21	68	6	26	0.96
$PO_{15.9}$	30	15.9	19.3	1.21	71	3	26	0.93
$PO_{15.0}$	30	15.0	19.5	1.29	71	4	25	0.89

Following functionalization to attach either hydrazides or aldehydes at the carboxylic acid functional groups, the polymers were again subjected to conductometric titration to determine what proportion of carboxylic acids had been converted. Conversion of the carboxylic acids in the $PO_{6.7}$ – $PO_{15.9}$ polymers to hydrazides occurred with ~55% efficiency irrespective of molecular weight (Table 3 – 3), resulting in similar mole fractions of grafted hydrazides in each polymer (14 – 15 %); given the different M_n values of the $POH_{6.7}$ – $POH_{15.9}$ polymers, this translated to between 5 – 12 hydrazide groups per polymer chain. The conversion of the carboxylic groups on the $PO_{15.0}$ polymer to aldehydes was slightly less efficient (~43%), translating to a ~10% mole fraction of aldehyde-containing monomer residues or ~8 aldehyde groups per chain (Table 3 – 3). We hypothesize that this difference is related either to the decreased efficiency of the EDC reaction in organic solvent or non-quantitative acetal deprotection to aldehydes following grafting. Thus, while hydrogels prepared with a 1:1 mass ratio of

hydrazide and aldehyde polymer would contain a ~16 – 20% molar excess of hydrazide groups, the similar degree of hydrazide functionalization in each different POH_n polymer prepared results in each gel produced exhibiting a fixed ratio of Hzd:Ald groups.

^{1}H-NMR of the functionalized polymers (run in DMSO) produced a spectrum with signals

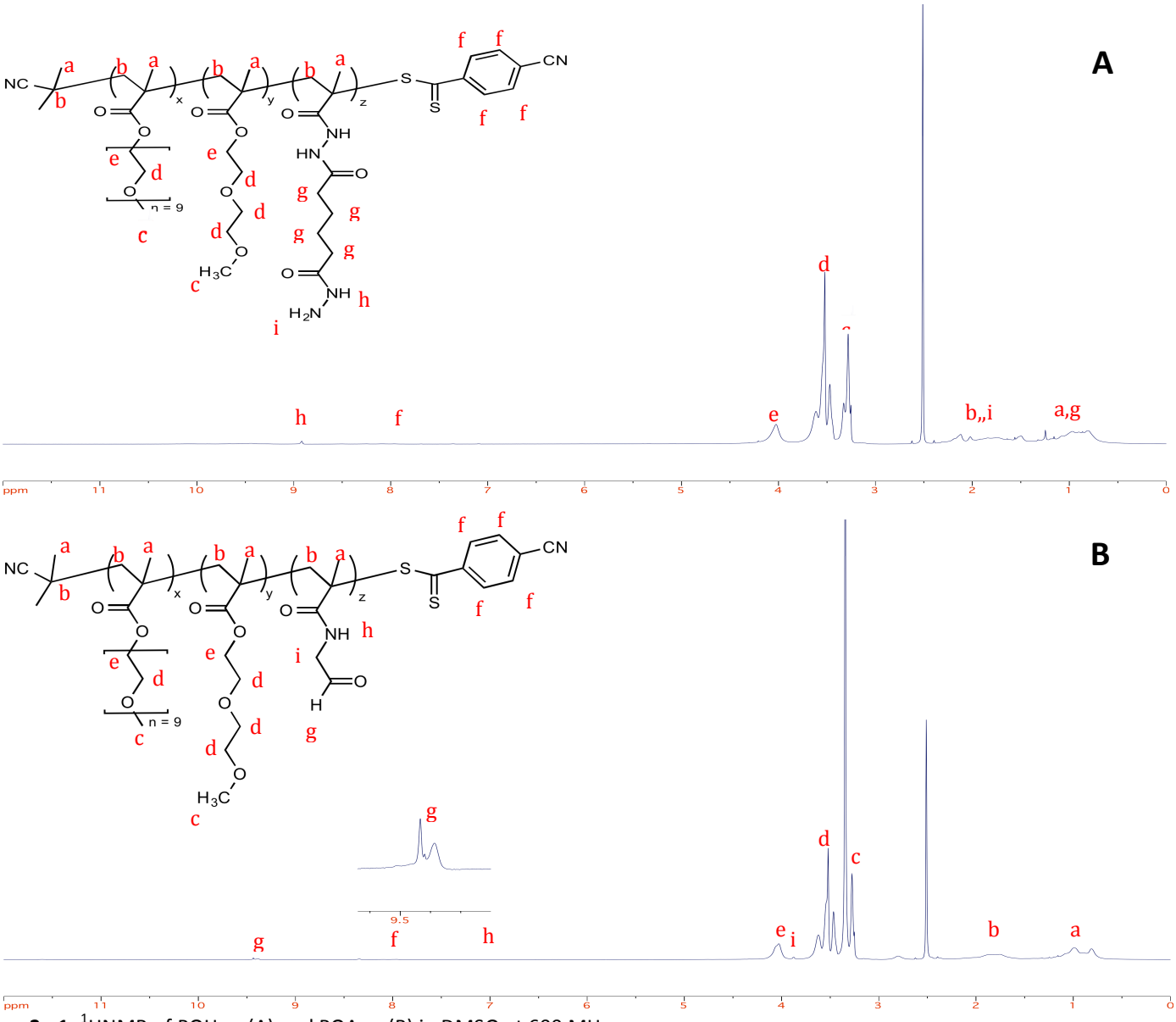

Figure 3 - 1. ^{1}HNMR of $POH_{15.9}$ (A) and $POA_{15.0}$ (B) in DMSO at 600 MHz.

closely matching those of POEGMA, and, in the case of $POA_{15.0}$, also showing an easily

distinguishable aldehyde peak (ppm = 9.5) indicating successful grafting of the aldehyde functional group (Fig. 3 – 1B).

Table 3 - 3. Characterization of functionalized POEGMA polymers.

Polymer	MAA Conversion (%)	Functional Monomer (mol %)	Functional groups (#/chain)	Cloud Point (°C)
$POH_{6.7}$	54	14	5	76
$POH_{9.3}$	54	15	7	79
$POH_{11.6}$	58	15	9	78
$POH_{15.9}$	54	14	12	79
$POA_{15.0}$	43	10	8	64

3.3.2 Preparation of *in situ* gelling injectable POEGMA hydrogels

A series of four different gels was prepared by pipetting various volumes (120 μl for swelling/degradation, 250 μl for rheological measurments) of a 150 mg/mL solution of one of the $POH_{6.7}$ – $POH_{15.9}$ polymers into a silicone mold (with volume equal to twice the volume of the POH_n polymer used) followed by pipetting an equal volume of a 150 mg/ml solution of $POA_{15.0}$ polymer and mixing by repeated pipetting (Fig. 3 – 2; Table 3 - 4). The complementary hydrazide/aldehyde functional groups on the reactive pre-polymers react upon mixing to form reversible covalent hydrazone bond cross-links, leading to gelation of all the gels in the series within time frames of < 1 minute. The gels

exhibited gelation rates that were directly related to the molecular weight of the POH_n precursor used to form the gel; gels formed with the lowest molecular weight $POH_{6.7}$ precursors took the longest to gel (~35 s) while gels formed with the highest molecular weight $POH_{15.9}$ precursors gelled most rapidly (~15s) (Table 3 – 4).

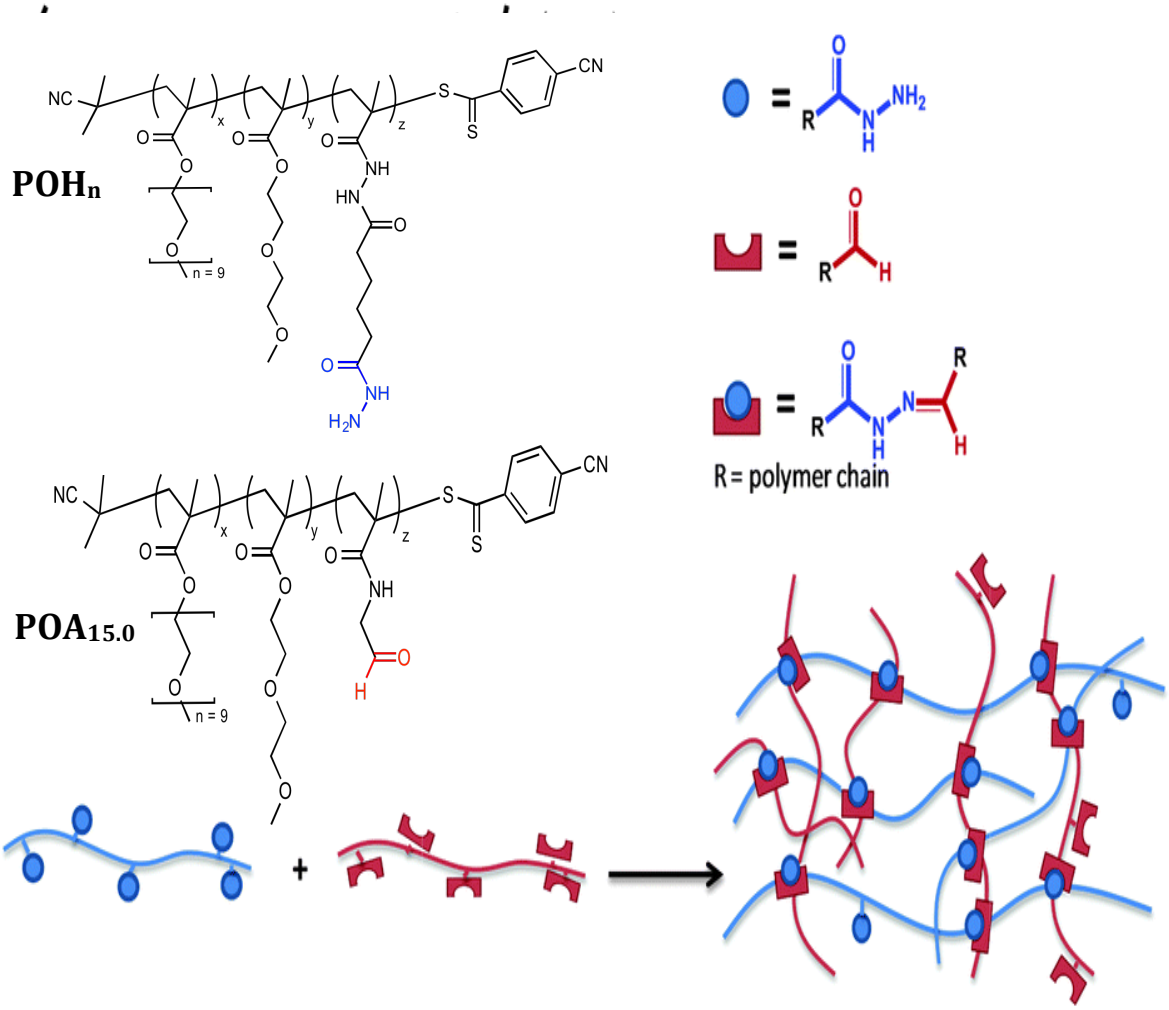

Figure 3 - 2. Schematic representation of the formation of covalently cross-linked hydrogels via mixing of hydrazide/aldehyde functionalized POEGMA precursors.

At the same functional group density (as is the case for these polymers), larger MW polymers will have more reactive functional groups per chain (Table 3 – 3); as a result,

each polymer chain will be able to form more cross-links with other polymers in solution and thus more rapidly approach the gel point at which the sol-gel transition occurs relative to smaller MW polymers with similar distributions of functional groups [104].

Table 3 - 4. Preparation of injectable POEGMA hydrogels.

Gel	Polymer Conc. (mg ml^{-1})	Gelation Time (s)
$POH_{6.7}/POA_{15.0}$	150/150	~35
$POH_{9.3}/POA_{15.0}$	150/150	~30
$POH_{11.6}/POA_{15.0}$	150/150	~25
$POH_{15.9}/POA_{15.0}$	150/150	~15

The transmittances of each of the hydrogels produced were >98% at 595 nm and >93% at 405 nm, with no significant differences between the mean transmittance of the gels at either wavelength ($p > 0.05$; Fig. 3 – 3). This result suggests the hydrogels are highly transparent, consistent with our previous results using chain transfer polymerization to prepare similar precursor polymers [88]. To determine if cross-links were formed at equal densities throughout all of the POEGMA hydrogels, the numbers of residual functional groups in gels prepared with different molecular weight polymer precursors were quantified by fluorescent labeling. The gels were immersed in solutions of hydrazide-reactive 5-FITC or aldehyde-reactive 5-FTSC and then extensively rinsed to remove non-reacted dye. Fluorescence analysis indicates that the concentration of unreacted hydrazides and aldehydes was the same ($p > 0.05$ in all pairwise comparisons) across all of the gels (Fig. 3 – 4).

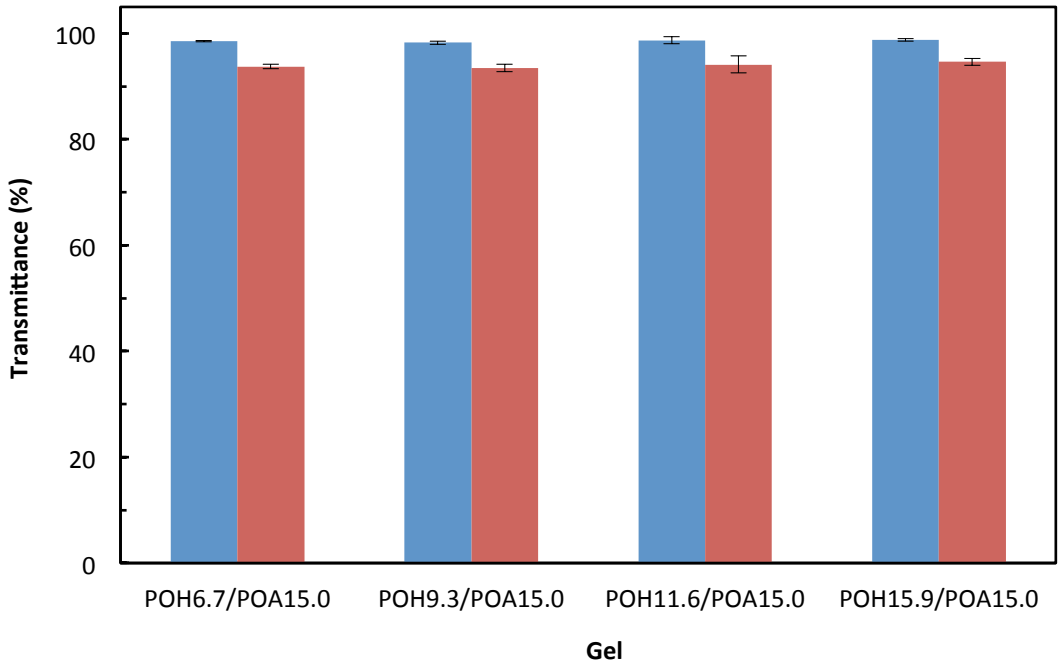

Figure 3 - 3. Transmittance of POEGMA gels in polystyrene tissue culture plates at 595 (blue) and 405 (red) nm wavelengths. Differences between mean transmittances were not statistically significant ($p > 0.05$ for all pairwise comparisons). Errors bar represent one standard deviation from the mean ($n = 3$).

This result is consistent with the similar number and (based on the same backbone monomer compositions) distributions of reactive functional groups present in the $POH_{6.7}$ to $POH_{15.9}$ polymers and indicates that each hydrazide polymer formed similar numbers of cross-links with the $POA_{15.0}$ polymer during hydrogel formation. Thus, from a compositional perspective, the four gels prepared are chemically identical aside from a slightly higher concentration of the RAFT agent in lower molecular weight polymers prepared with higher CPCDB contents.

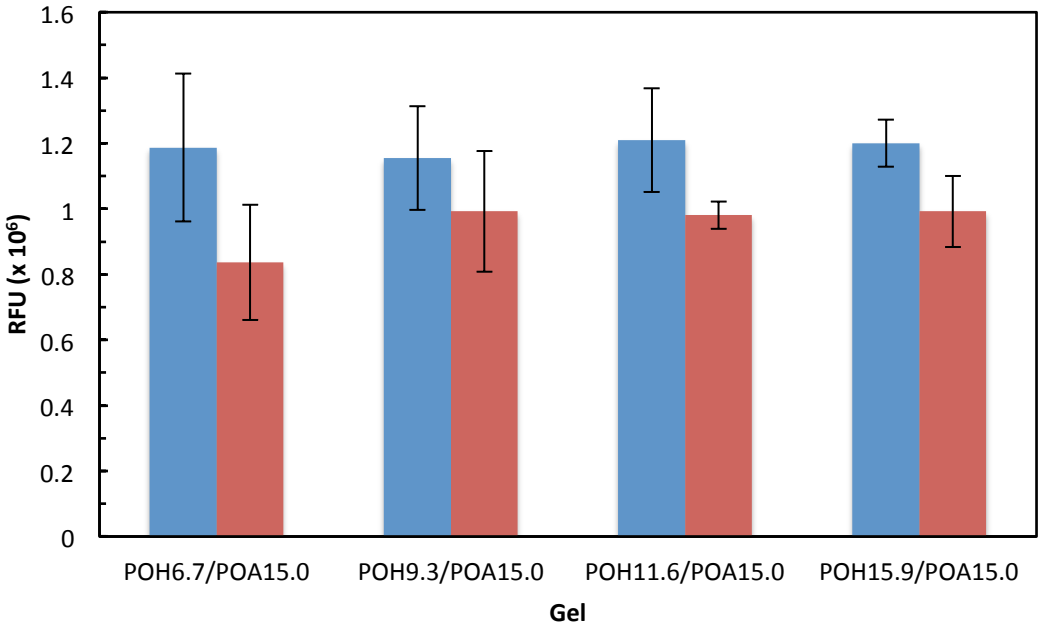

Figure 3 - 4. Relative fluorescence readings of 5-FITC (blue) and 5-FTSC (red) bound to unreacted hydrazide and aldehyde groups respectively in POEGMA gels. Error bars represent one standard deviation from the mean (n = 3). Differences between mean fluorescence readings were not significant ($p > 0.05$ in pairwise comparisons).

3.3.3 Swelling and Degradation Kinetics

The swelling kinetics of the POEGMA gels were assessed in 10 mM PBS at 22 °C, with all gels normalized to an initial weight to track the swelling ratio (SR; Fig. 3 – 5A). All of the POEGMA gels showed similar swelling patterns over the length of the experiment (2 weeks), swelling over the first 24h followed by a plateau in swelling up to 32h and then a slow reduction in mass over the course of the experiment; this later time mass loss is attributable to the slow degradation of hydrazone bonds in aqueous solution, which led to expansion of the hydrogel network and increased water uptake. There were however, marked differences in the rates and degrees of swelling between the POEGMA gels, with gels prepared with lower molecular weight precursor polymers

consistently swelling more at each time point tested. Of note, the differences in swelling appear to be accentuated particularly at the lower molecular weight end of the precursor polymers studied, with the difference in swelling between the $POH_{6.7}/POA_{15.0}$ and $POH_{9.3}/POA_{15.0}$ gels significantly higher than that between the $POH_{11.6}/POA_{15.0}$ and $POH_{15.9}/POA_{15.0}$ gels. Furthermore, the gels made with lower molecular weight precursors ($POH_{6.7}/POA_{15.0}$ and $POH_{9.3}/POA_{15.0}$) swelled at a slower rate than gels that were made with higher molecular weight precursors ($POH_{11.6}/POA_{15.0}$ and $POH_{15.9}/POA_{15.0}$; Table 3 – 5) but also swelled to higher maximum swelling ratios. To further characterize the stability of these gels over time, swelling and degradation studies were performed in both 10 mM PBS (physiological model conditions) and 10 mM HCl (accelerated conditions) at 37 °C. In 10 mM PBS, the gels behaved similarly at 37 °C as they did at 22 °C over the initial 24 h swelling period, consistent with the lack of a thermal phase transition in these POEGMA gels and the minimal degradation that occurs over the first day of incubation. However, after the 24 h time point, the gels swelled more than observed at 22 °C (likely due to accelerated degradation of hydrazone bonds at 37 °C), although at the same relative rates observed at 22 °C (Fig. 3 – 5B). However, starting at 48 h for $POH_{6.7}/POA_{15.0}$, the observed swelling ratio reaches a maximum, after which SR rapidly decreased in the subsequent 24 h until no gel remained in the insert (i.e. a complete gel-sol transition has occurred that enabled facile wash-out of the polymers from the porous inserts). The time required for the gels to reach the point of gel-sol transition directly correlated with the molecular weight of the POH_n polymer used to make the gel.

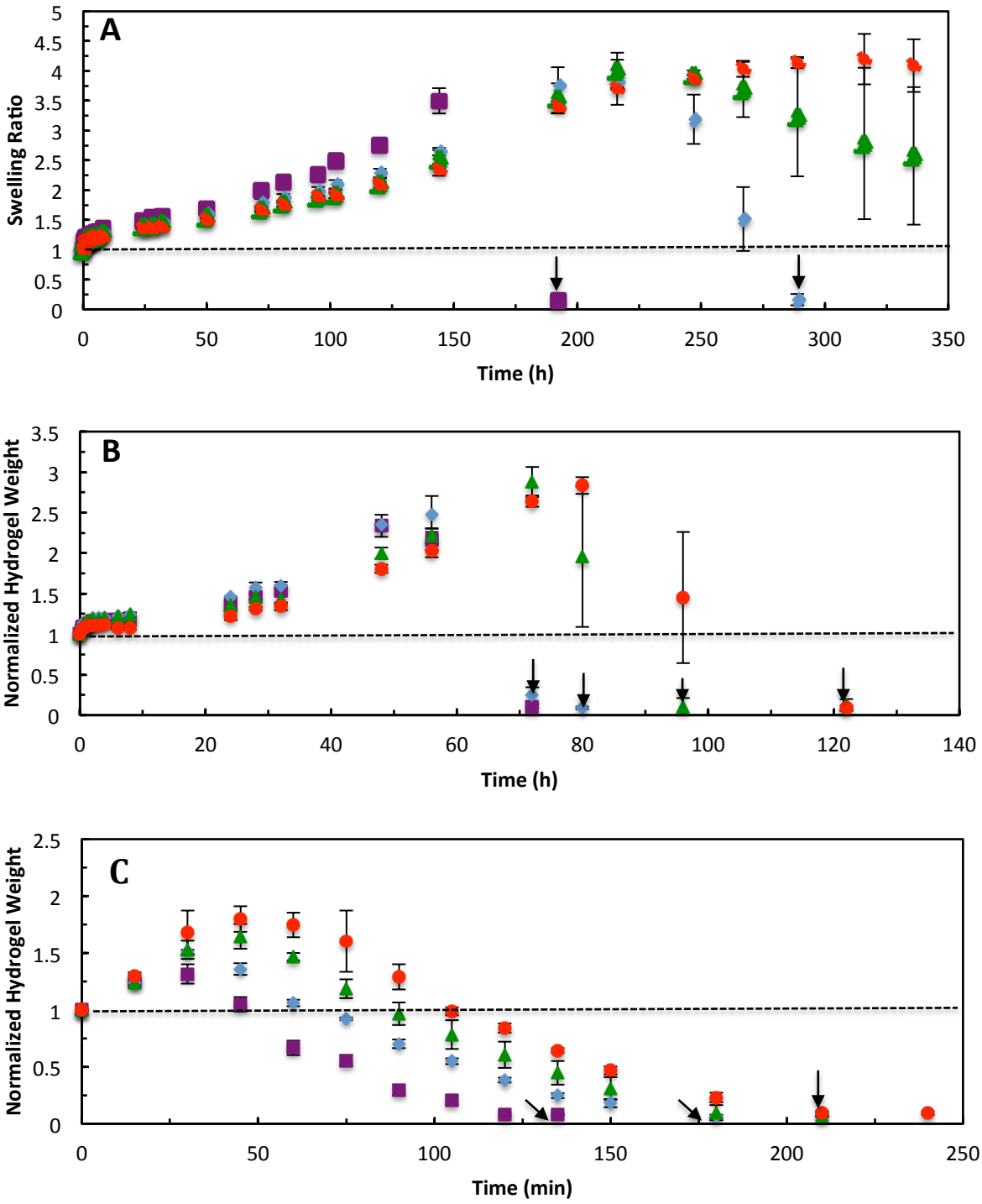

Figure 3 - 5. Swelling and degradation kinetics of $POH_{6.7}/POA_{15.0}$ (purple square), $POH_{9.3}/POA_{15.0}$ (blue diamond), $POH_{11.6}/POA_{15.0}$ (green triangle), and $POH_{15.9}/POA_{15.0}$ (red circle) POEGMA hydrogels. (A) Swelling at 22 °C in 10 mM PBS. (B) Swelling and degradation at 37 °C in 10 mM PBS. (C) Accelerated degradation at 37 °C in 10 mM HCl. Arrows indicate time points at which the gel had degraded sufficiently to be easily washed out of the inserts. Error bars represent one standard deviation from the mean (n=3).

Under both physiological and acid-catalyzed conditions; hydrogels prepared with higher molecular weight precursor polymers continued to swell prior to degradation for longer periods of time. Again, given the identical cross-link density in each gel (Fig. 3 – 4), this result can be attributed to the additional chain ends present in hydrogels prepared with lower molecular weight precursor polymers, effectively representing one less cross-link that must be broken to induce a gel-sol transition.

Table 3 - 5. Swelling kinetics of POEGMA hydrogels in 10 mM PBS at 22 C.

Gel	SR	k^a
$POH_{6.7}/POA_{15.0}$	1.48 ± 0.01	1.22 ± 0.01
$POH_{9.3}/POA_{15.0}$	1.41 ± 0.06	1.14 ± 0.01
$POH_{11.6}/POA_{15.0}$	1.41 ± 0.03	1.58 ± 0.01
$POH_{15.9}/POA_{15.0}$	1.35 ± 0.02	1.98 ± 0.01

[a] *k* is determined after 8 hours.

Similar trends in degradation were noted when the gels were incubated in 10 mM HCl at 37 °C (Fig. 3 – 5C), although complete degradation in all gels was achieved in three hours or less owing to the acid-catalyzed mechanism of hydrazone degradation [105] while degradation in physiological conditions could be tuned from ~1 week ($POH_{6.7}/POA_{15.0}$) to > 2 weeks ($POH_{15.9}/POA_{15.0}$) according to the molecular weight of the precursor polymer used.

3.3.4 Rheology

The mechanical properties of the hydrogels were assessed under both shear and compressive stress to correlate gel properties with the precursor polymer properties (Figure 3 – 6). The average G' of each hydrogel over a range of frequencies within the linear viscoelastic region was directly related with the molecular weight of the hydrazide POH_n precursor polymer used to form the gel (Fig. 3 – 6A), with an exponential relationship (R^2 = 0.98) observed between the molecular weight of the precursor polymers and the shear modulus of the resulting hydrogel (Fig. 3 – 6B). Similarly, the compressive modulus of the hydrogels generally increases as the molecular weight of the precursor polymer increases (Fig. 3 – 6B), again in a non-linear fashion with higher modulus changes observed primarily with the higher molecular weight polymer precursors studied; indeed, under compression, only the $POH_{15.9}$/$POA_{15.0}$ gel had a modulus that was significantly different from the others at 95% confidence. Thus, while the number of crosslinked functional groups (Fig. 3 – 4) and the basic chemical composition (Table 3 – 3) of each hydrogel is equivalent, the mechanics of the gels can be controlled based on the molecular weight of the precursor polymers used to prepare the gels.

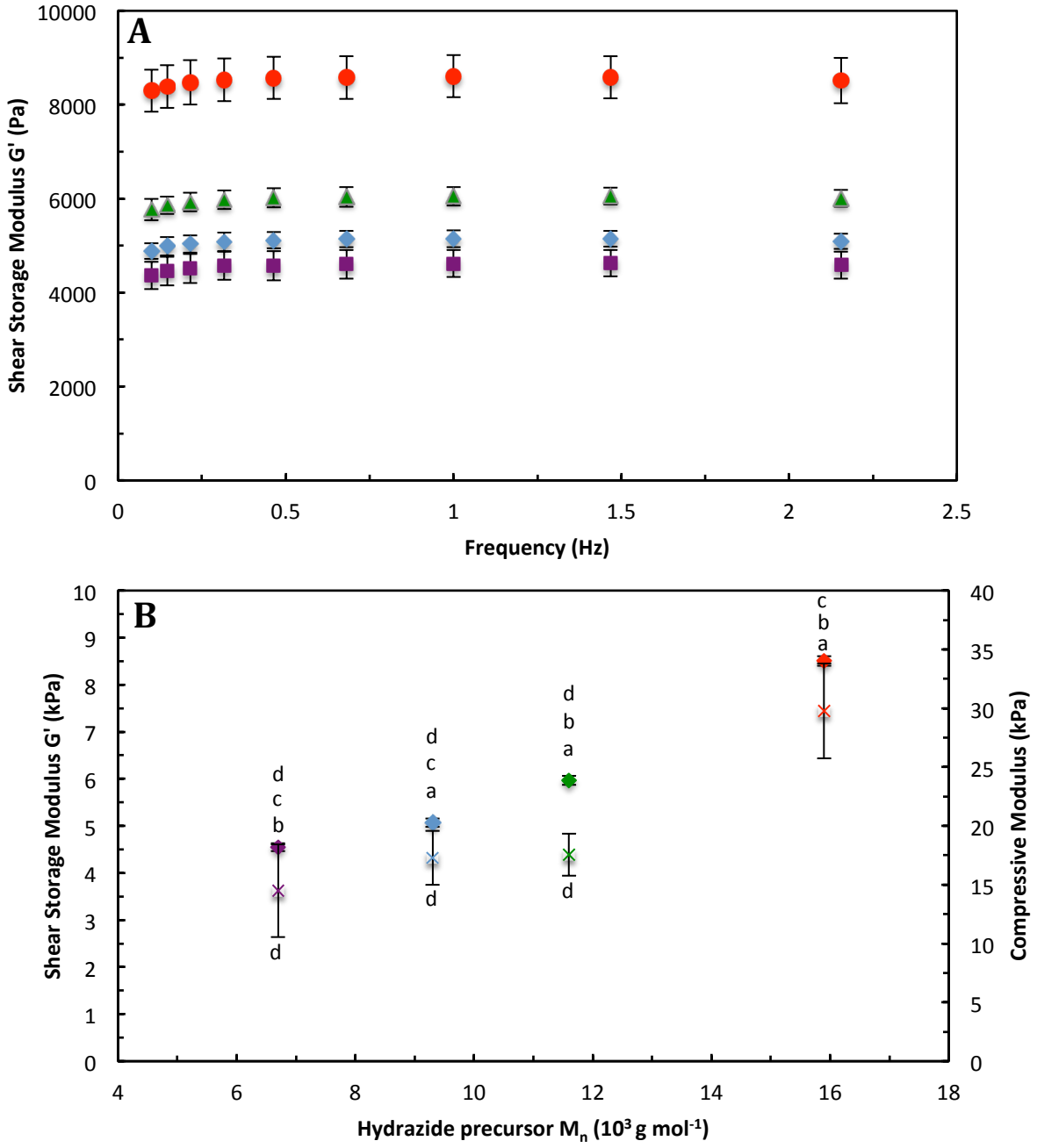

Figure 3 - 6. Rheological properites of POEGMA hydrogels. (A) Shear storage modulus of $POH_{6.7}/POA_{15.0}$ (purple square, a), $POH_{9.3}/POA_{15.0}$ (blue diamond, b), $POH_{11.6}/POA_{15.0}$ (green triangle, c), and $POH_{15.9}/POA_{15.0}$ (red circle, d) POEGMA hydrogels over a frequency sweep (0.1 – 2.1 Hz) within each gel's LVE; (B) Average compressive modulus (unfilled points, right axis, letter below marker = $p < 0.05$ in pair-wise comparison with respective gel) and shear modulus (filled points, left axis, letter above marker = $p < 0.05$ in pair-wise comparison with respective gel) of POEGMA hydrogels as a function of the M_n of the POH_n precursor used to make the gels. Error bars represent one standard deviation from the mean (n = 3)

3.3.5 *In vitro* cytoxicity of POEGMA gel precursors

The cytotoxocities of the $POH_{6.7}$ – $POH_{15.9}$ and $POA_{15.0}$ polymers were assessed using a resazurin assay on 3T3 mouse fibroblasts. The results of the assay indicate that none of the polymers exhibited significant cytotoxicity ($p > 0.05$ in pairwise comparisons with the control; Fig. 3 – 7), even up to concentrations of 2 mg ml^{-1}; note that this represents an extremely high concentration to be assessed in an *in vitro* cytotoxicity assay. These results are also consistent with the cytotoxicities of functionalized POEGMA polymers prepared with standard chain transfer polymerization in our group [90], suggesting that neither the use of lower molecular weight precursor polymers nor the use of RAFT for preparing the polymers has any significant impact on the cytotoxicity of the resulting materials.

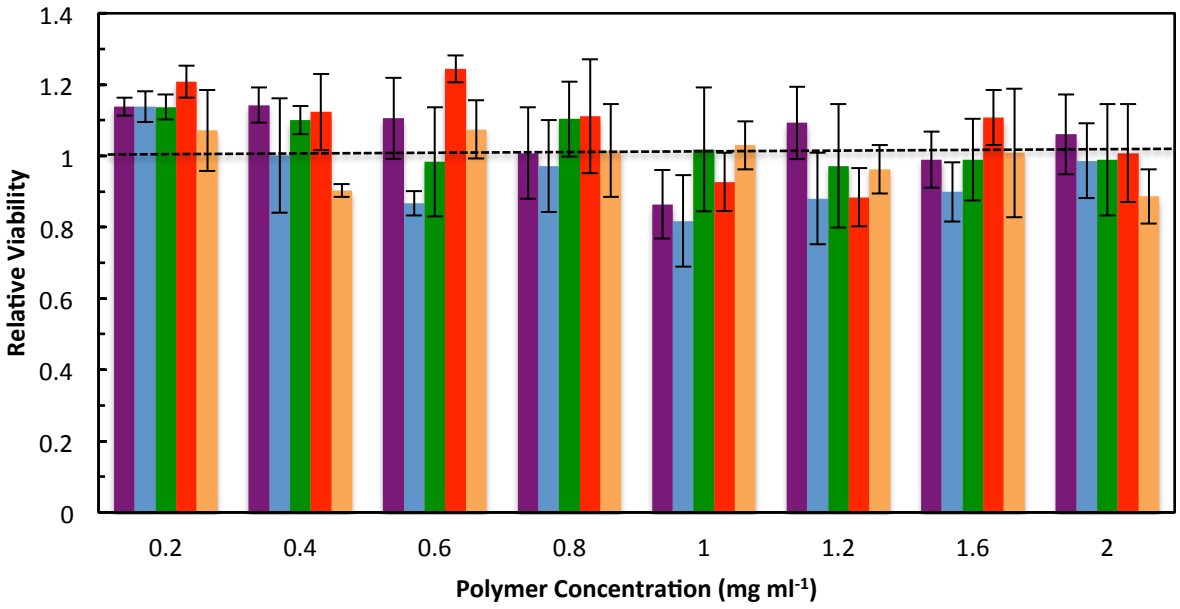

Figure 3 - 7. Relative viability of 3T3 mouse fibroblasts treated with with $POH_{6.7}$ (purple), $POH_{9.3}$ (blue), $POH_{11.6}$ (green), $POH_{15.9}$ (red) and $POA_{15.0}$ (orange) at concentrations ranging from 0.2 – 2 mg ml^{-1} for 24 hours. Error bars represent one standard deviation from the mean (n = 4)

3.4 Conclusions and Future Work

RAFT chemistry and subsequent post-polymerization functionalization was used to prepare a series of well-defined hydrazide and aldehyde-functionalized POEGMA polymers with M_n values ranging from 6.7 to 15.9 kDa but chemically equivalent in terms of both the mole fractions of the constituent monomers and the density of reactive functional groups. Hydrogels prepared with precursor polymers with higher molecular weights produced gels that formed faster, exhibited higher compressive and shear moduli, degraded more slowly, and swelled more slowly and to lower maximum swelling capacities than gels prepared with lower molecular weight precursor polymers, although the number of functional covalent hydrazone bonds formed in all cases was observed to be equivalent; as such, it is the molecular weight of the gel precursors and, more specifically, the presence of a higher density of polymer chain ends per unit volume that drives the observed changes in gel properties independent of any significant chemical differences between the gels.

The results of this study indicate that the properties of injectable hydrogels can be effectively controlled by varying the molecular weights of the precursor polymers used to make the gels *without* significantly changing the chemistry of the precursor polymers or, by virtue of the similar covalent cross-link densities of each hydrogel formed, the chemistry of the resulting hydrogels. This opens up interesting possibilities for both engineering hydrogel scaffolds with more precise drug delivery/tissue engineering properties and/or more effectively decoupling the effects of mechanics and chemistry on the responses of cells to their substrates. In particular, we anticipate that

such hydrogels have significant potential for effectively isolating the effect of substrate stiffness on directing the growth and differentiation of stem cells on hydrogel substrates, which is challenging to unambiguously identify with current approaches to modifying synthetic hydrogel mechanics [106-108].

We anticipate particular applications of such chemistry-independent control over gel properties in terms of precisely tuning diffusive drug delivery kinetics without altering partitioning-driven changes in release kinetics and/or decoupling the effects of mechanics and interfacial chemistry on the behaviour of cells at interfaces.

Acknowledgements

The Natural Sciences and Engineering Research Council of Canada (NSERC) is acknowledged for funding this work.

4 Controlled synthesis of functionalized hyperbranched POEGMA polymers with tunable branching for use in the preparation of injectable hydrogels

4.1 Introduction

Hyperbranched polymers (HBPs) have attracted significant recent attention as potential precursors for use in the preparation of hydrogels for a variety of drug delivery and cell encapsulation applications [109]. The unique nanoscale structure and globular molecular structure of hyperbranched polymers give them a number of properties that make them favourable for these types of applications [110], with their high peripheral functionality and functional group accessibility particularly useful to promote improved reactivity and drug loading efficiency as compared to their linear polymers [111].

Most commonly, in the context of hydrogels, HBPs have been combined with linear polymers or proteins to improve the stability, mechanical strength, and/or functional group accessibility within a hydrogel [112]. As an example from the functionalization perspective, Hassan et al. showed extended viability and conserved cellular behavior (e.g. cytokine and growth factor secretion) of human adipose-derived stem cells (hADSCs) encapsulated in hyperbranched-PEG/linear hyaluronic acid (HA) hydrogels, with the presence of many functional groups at the periphery of the hyperbranched polymers demonstrated to the key to allow for extensive post-polymerization functionalization with proteins and other cell-signaling molecules [113]. As an example from the crosslinking/mechanics perspective, Liu *et al.* demonstrated the use of hyperbranched phosphoramidate/linear HA hydrogels to produce injectable

hydrogels for controlled protein release, exploiting the potential of hyperbranched polymers to form multiple localized crosslinks to regulate protein release kinetics [114]. Dong *et al.* also produced an injectable hydrogel based on hyperbranched PEG that could form gels *in situ* via thiol-ene "click" chemistry [109]. Furthermore, relative to other types of highly branched molecules such as dendrimers, the synthetic route to form hyperbranched polymers is relatively easy, often via "one-pot" methods without the need for the multiple isolation and purification steps required for dendrimer synthesis [115]. In the case of monomers with vinyl functionalities, HBPs are typically prepared simply via the inclusion of di-functional cross-linkers in a linear polymer recipe. Ostensibly, the degree of branching in such a system can be controlled simply by varying the mol% of cross-linker included in the reaction mixture. However, the concentration of cross-linker must be controlled such that it does not exceed the gel point for a particular polymer system and the HBPs remain soluble throughout the course of this reaction [116]. Including a chain transfer agent is one commonly employed method for limiting the amount of gel formation. The chain transfer agent added may be a traditional chain transfer agent used to control linear polymer molecular weight in free radical polymerization (e.g. 1-dodecanethiol [117], N,N-tetraethylthiuram disulfide [118]); the chemistry of that agent can be chosen to incorporate desired chemistry at the chain ends of the branches formed. Alternately, a RAFT agent may be used as the chain transfer agent to both facilitate solubility and mediate additional polymerization, with parameters such as temperature and RAFT-agent concentration useful to tune size and branching degree in the final HBPs produced [119-121]. Thus, RAFT is a versatile

technique that can effectively control HBP production with a range of both backbone monomers (including OEGMA-based monomers) [58, 122] and di-vinyl cross-linkers. However, while synthetic hyperbranched polymers have previously been used as building blocks in *in situ* gelling hydrogels [113, 123], to our knowledge no studies have investigated how systematically varying the degree of branching of HBPs affects their properties, both in terms of the polymerization kinetics involved as well as their functionality as precursors for the formation of injectable hyperbranched-linear hybrid hydrogels. Furthermore, no study has described a system for the formation of *in situ* gelling hybrid hydrogels that functions without the need for the inclusion of additional cross-linker to induce gelation.

In this study, a series of POEGMA polymers with various degrees of branching was prepared via RAFT polymerization of a combination of oligoethylene glycol methacrylate ($OEGMA_{475}$), methacrylic acid (MAA), and ethylene glycol dimethacrylate (EGDMA). The polymers were characterized to determine how changing the degree of branching affects the structural properties of these polymers as well as their polymerization kinetics. The polymers were then functionalized with hydrazide groups at the carboxylic acid sites and mixed with linear aldehyde-functionalized POEGMA to form hyperbranched-linear hybrid hydrogels (Fig. 4 – 1).

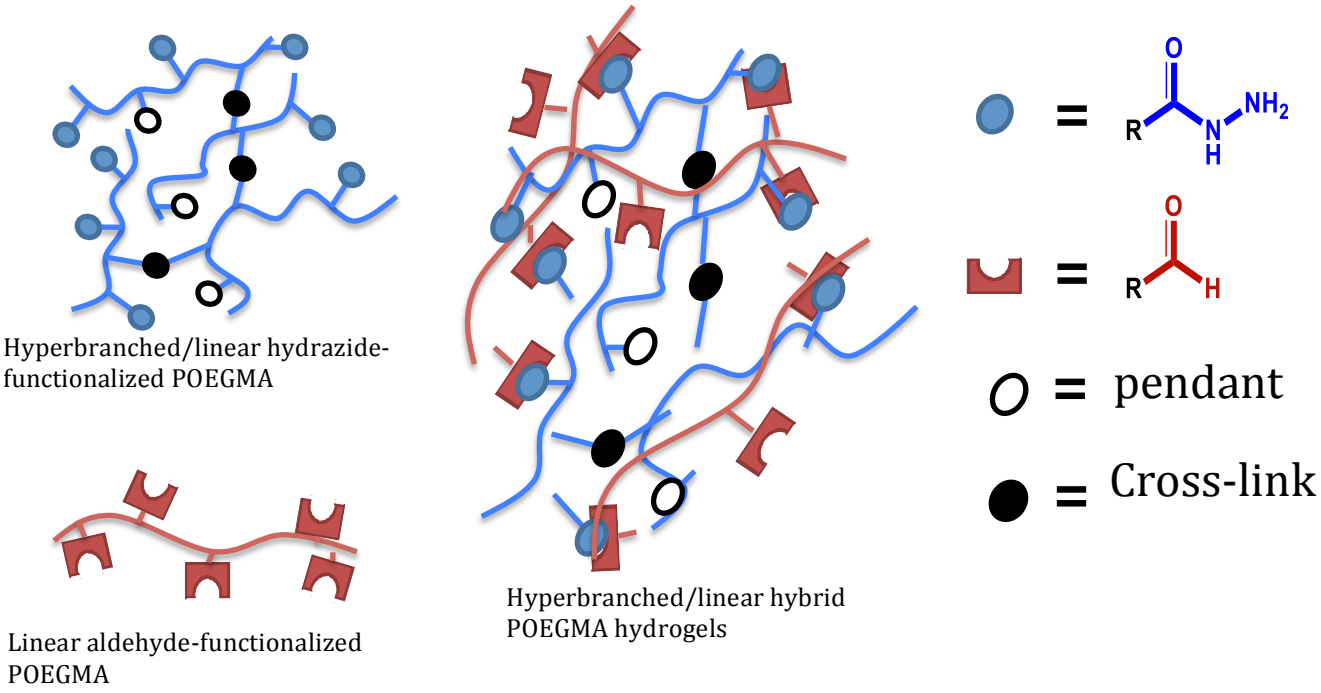

Figure 4 - 1. Schematic of the preparation of hyperbranched/linear hybrid hydrogels by mixing of hydrazide-functionalized hyperbranched/linear POEGMA precursors and linear aldehyde-functionalized POEGMA precursor.

4.2 Materials & Methods

4.2.1 Materials

All chemicals were purchased from Sigma Aldrich (Oakville, ON) unless otherwise noted. Ethylene glycol dimethacrylate (EGDMA; Sigma Aldrich, Oakville ON) was passed through a column of basic aluminum oxide (Sigma Aldrich, type CG-20) to remove the methyl ether hydroquinone inhibitor prior to use. Di(ethylene glycol) methyl ether methacrylate ($M(EO)_2MA$, 95%), oligo(ethylene glycol) methyl ether methacrylate ($OEGMA_{475}$, 95%) with an average molecular weight of 475 g mol^{-1}, and methacrylic acid (MAA, 99%) were purified via passage over a column of basic aluminum oxide (type CG-20) to remove the methyl ether hydroquinone (MEHQ) and butylated hydroxytoluene

(BHT) inhibitors. Azobisisobutyronitrile (AIBN, 95%), 2-cyano-2-propyl 4-cyanobenzodithioate (CPCDB, 98%), adipic acid dihydrazide (ADH, Alfa Aesar, 98%), N'-ethyl-N-(3-dimethylaminopropyl)-carbodiimide (EDC, Carbosynth, Compton CA, commercial grade), aminoacetaldehyde dimethyl acetal (ADA, 99%), and N-hydroxysuccinimide (NHS, 98%) were used as received. 3T3 *Mus musculus* mouse cells were obtained from ATCC: Cedarlane Laboratories (Burlington, ON). Dulbecco's modified Eagle medium (+glucose, +pyruvate, DMEM), fetal bovine serum (FBS), penicillin/streptomycin (PS), and trypsin-ethylenediaminetetraacetic acid were purchased from Invitrogen Canada (Burlington, ON). 1,4-Dioxane (reagent grade), dichloromethane (DCM, reagent grade), and diethyl ether (reagent grade) were purchased from Caledon Laboratory Chemicals (Georgetown, ON). Hydrochloric acid (HCl, 1M) was received from LabChem Inc. (Pittsburgh, PA). Milli-Q grade distilled deionized water (DIW) was used for all experiments.

4.2.2 Polymer synthesis

4.2.2.1 Synthesis of hydrazide-functionalized hyperbranched POEGMA polymers (PO_n-H)

A series of four hyperbranched POEGMA polymers was prepared with various targeted degrees of branching ranging from 0 – 15% (PO_{15}, PO_{10}, PO_5, and PO_0; where the subscript represents the targeted degree of branching). In a typical reaction (PO_{15}), $OEGMA_{475}$ (5 g), EGDMA (0.57 g), MAA (0.495 g), and AIBN (10.5 mg) were mixed together and dissolved in 25 ml of 1,4-dioxane. The DB of the other HBPs prepared was varied by changing the mol% of EGDMA included in the reaction mixture from 0 – 15

mol% and correspondingly lowering the $OEGMA_{475}$ mole fraction in the recipe; see Table 4 – 1 for full recipes. CPCDB (55.4 mg) was added to this solution, after which the solution was transferred to a sealed Schlenk flask, degassed via three freeze-pump-thaw cycles, and backfilled with N_2. The flask was then submerged in a preheated oil bath at 70 °C, and the mixture was allowed to react for 9h. Samples were taken from the reaction at predetermined time intervals for GPC and NMR analysis. After 9h, the reaction was stopped by submerging the reaction vessel in an ice bath and exposing the reaction to air; samples were taken of the crude reaction mixture to facilitate NMR analysis of conversion and GPC analysis of MW growth over time, and the remaining mixture was then precipitated in 10x cold ethyl ether. Samples of the (purified) precipitate were analyzed via GPC, NMR and conductometric titration to characterize the base hyperbranched polymer.

To prepare hydrazide-functionalized hyperbranched polymers, the remaining precipitate from the previous step was dissolved in 100 ml of deionized water to which ADH (10.03 g) was added. The pH of the solution was lowered to 4.75 by addition of 1 M HCl, and 3.13 g of EDC was subsequently added. The pH of the solution was maintained at 4.75 by addition of 1 M HCl and 1 M NaOH as necessary for 4 – 5h (until the pH of the solution no longer changed). The reaction was subsequently allowed to stir overnight, after which the solution was transferred to 3.5 kDa regenerated cellulose tubing and dialyzed against deionized H_2O for 6 cycles (6 hours each). The solution was then lyophilized to dryness to yield the final product, which resembled a clear wax. The product was dissolved at 250 mg ml^{-1} in 10 mM PBS and stored at 4 °C.

Table 4 - 1. Synthesis of PO_{15} - PO_0 hyperbranched/linear POEGMA polymers.

Polymer	[OEGMA]/ [EGDMA]/ [MAA] Mole Fraction	[Monomer+ EGDMA]/ [CPCDB]/[AIBN] Mole Fraction	$M_{n,\ theory}$ (kDa)	DB_{theory} (%)
PO_{15}	55/15/30	1/85/300	26.9	15
PO_{10}	60/10/30	1/85/300	28.1	10
PO_5	65/5/30	1/85/300	29.3	5
PO_0	70/30	1/85/300	30.5	0
PO_0 (for aldehyde)	70/30	1/85/300	30.5	0

4.2.2.2 Synthesis of aldehyde-functionalized linear POEGMA (PO_0-A)

Aldehyde-functionalized linear POEGMA (PO_0-A) was prepared for use as the complementary polymer for preparation of injectable hydrogels with the hyperbranched hydrazide-functionalized POEGMA described above. $OEGMA_{475}$ (4.77 g), MAA (0.384 g), AIBN (7.875 mg), and CPCDB (41.55 mg) were dissolved in 18 ml of 1,4-dioxane and transferred to a sealed Schlenk flask. The solution was degassed via three freeze-pump-thaw cycles and then backfilled with N_2. The reaction vessel was subsequently submerged in a preheated oil bath at 70 °C and allowed to react under magnetic stirring (RPM = 350) for 9h. After 9h, the reaction was stopped by immersing the reaction vessel in an ice bath and exposing the reaction to air. Samples of the crude mixture were taken for NMR analysis to assess monomer conversion, with the residual product then isolated

by precipitation of the reaction solution into 10x cold ethyl ether. The precipitate was dried under vacuum for 4+ hours, and samples of the dried precipitate were used for analysis by NMR, GPC, and conductometric titration.

To functionalize the base polymer with aldehyde groups, the precipitate was dissolved in 50 ml of dichloromethane, after which 1.03 g of NHS and 1.38 g of EDC was also added to the solution. The reaction was allowed to proceed under stirring for 6h to activate the polymer with NHS, after which 1.41 g of ADA was added and the solution was stirred for another 24h. Dichloromethane was then removed by rotary evaporation, and the remaining polymer was dissolved in 150 ml H_2O. Excess reactants were removed by 2 cycles of dialysis in 3.5 kDa regenerated cellulose tubing against DI H_2O (at least 6 hours per cycle). The solution was then transferred to an Erlenmeyer flask, and 50 ml of 1 M HCl was added to hydrolyze the acetal groups of ADA to aldehydes. This reaction was allowed to stir for 48h, and the reaction was then purified via dialysis for 6 cycles of at least 6 hours each. The mixture was subsequently lyophilized to dryness to yield the final product, which resembled a clear wax. The product was dissolved to a concentration of 250 mg ml^{-1} in 10 mM PBS and stored at 4 °C.

4.2.3 Characterization of hyperbranched and linear POEGMA polymers

Size exclusion chromatography (SEC), ^{1}H-NMR, and conductometric titration were performed on both linear and hyperbranched POEGMA polymers at various stages during and after synthesis, according to the methods outlined in section 3.2.3. Aqueous SEC was performed in 25 mM CHES buffer (pH 10) on the PO_{15} – PO_0 samples taken from the synthesis reactions at 2, 4, 6, and 9 h time points in order to track the growth of the

polymers over the course of the reaction. ^{1}H-NMR was also performed on these samples in d_6-DMSO using a 600 MHz AVANCE spectrometer (Bruker). Conversion was estimated by comparing the vinyl peaks from unincorporated monomers against the peaks from the polymer backbone according to Eq. 3 – 2. The degree of branching was determined from the NMR data by using Equations 4 – 1 to 4 – 4, where upper case letters represent adjusted integral values for each monomer (R = branch points, P = pendant groups, A = MAA (as determined independently via base-into-acid conductometric titration), and M = $OEGMA_{475}$); f, c, e refer to peaks in the ^{1}H-NMR spectra as seen in Figure 4 – 1.

$$f = P \qquad \text{Eq. 4 - 1}$$

$$c = 3M \qquad \text{Eq. 4 - 2}$$

$$e = 4P + 4R + 2M \qquad \text{Eq. 4 - 3}$$

$$\%DB = (R/(P+R+A+M)) \times 100\% \qquad \text{Eq. 4 - 4}$$

Conductometric titrations were performed on the polymers following the synthesis reaction (to quantify MAA content of the base polymers), and following functionalization (to quantify the percentage conversion of MAA groups to hydrazide or aldehyde groups).

4.2.4 Preparation of *in situ* gelling POEGMA hydrogels

A series of four hyperbranched-linear hybrid POEGMA hydrogels (G_{15}, G_{10}, G_5, and G_0) were prepared by mixing one of the hydrazide-functionalized POEGMA polymers (PO_{15}-H – PO_0-H) with the linear aldehyde-functionalized POEGMA. Stock

solutions of polymer at 25% w/v were diluted down to a working concentration of 20% w/v in 10 mM PBS. 120 µl of one of the PO_n-H polymer solutions was pipetted into a silicone rubber mold (r = 9 mm), along with an equal volume of PO_0-A polymer solution. The solutions were mixed via vigorous manual stirring over 5 – 10 seconds with a 1 ml pipette and allowed to gel in a sealed, humid container (RH = 100%) overnight. Gelation was subsequently confirmed by removal of the solid POEGMA hydrogels from the rubber molds.

4.2.5 Cell viability assay

The cytotoxicities of the PO_{15} – PO_0-H hyperbranched/linear polymers and the PO_0-A linear polymers were determined via a resazurin fluorescence assay that was conducted on 3T3 mouse fibroblasts, according to the method outlined in section 3.2.7. The cytotoxicities of the polymers were assessed at concentrations ranging from 200 to 2000 µg ml^{-1}. The fluorescence readings from experimental wells were compared against those from a media-only control (no cells or polymer) and a cell-only control (no polymer) to determine relative cell viability. Error bars represent one standard deviation from the mean of the measured cell viability percentages (n = 4).

4.3 Results

4.3.1 Synthesis and characterization of hyperbranched POEGMA polymers

A series of four hydrazide-functionalized hyperbranched/linear POEGMA polymers (PO_{15}-H – PO_0-H) were prepared with targeted degrees of branching ranging from 0 to 15% in addition to a linear aldehyde-functionalized polymer (PO_0-A) to be

used as a complementarily functionalized polymer for *in situ* hydrogel formation (Fig. 4 – 2). The PO_{15}-H - PO_0-H series of polymers was prepared via RAFT to control the DB such that it did not exceed the gel point during polymerization, maintaining solubility for each of the hyperbranched polymers prepared. In general, the DB of the PO_{15}-H - PO_0-H polymers closely matched the mol% of EGDMA that was included in the reaction, with each experimental product exhibiting a degree of branching just slightly below the theoretical target (Table 4 – 2). This slightly lower branching degree is likely attributable to the presence of pendant vinyl groups on cross-linkers that were incorporated into the polymer but did not form a branch point with another polymer chain.

Table 4 - 2. Characterization of unfunctionalized hyperbranched/linear POEGMA polymers.

Polymer	M_n (kDa)	M_w (kDa)	Đ	Conversion
PO_{15}	22.6	51.3	2.27	0.83
PO_{10}	19.8	35.6	1.80	0.81
PO_5	15.6	21.2	1.36	0.81
PO_0	13.9	16.7	1.20	0.67
PO_0 (for aldehyde)	14.5	17.7	1.22	0.74

In each hyperbranched polymer tested, EGDMA was incorporated in slightly larger than stoichiometric proportions, indicating that the transfer constant for CPCDB with respect to EGDMA may be slightly higher than it is for $OEGMA_{475}$. Samples of each polymerization reaction were taken at 2, 4, 6, and 9h time points and analyzed via GPC and NMR to track the size and conversion of the polymer over time. Nine hours was

chosen as the reaction termination time point because it was experimentally determined that longer polymerizations (in the case of the most highly branched polymers) yielded polymers that were too large to remain soluble following functionalization, making them inefficient for use as hydrogel building blocks.

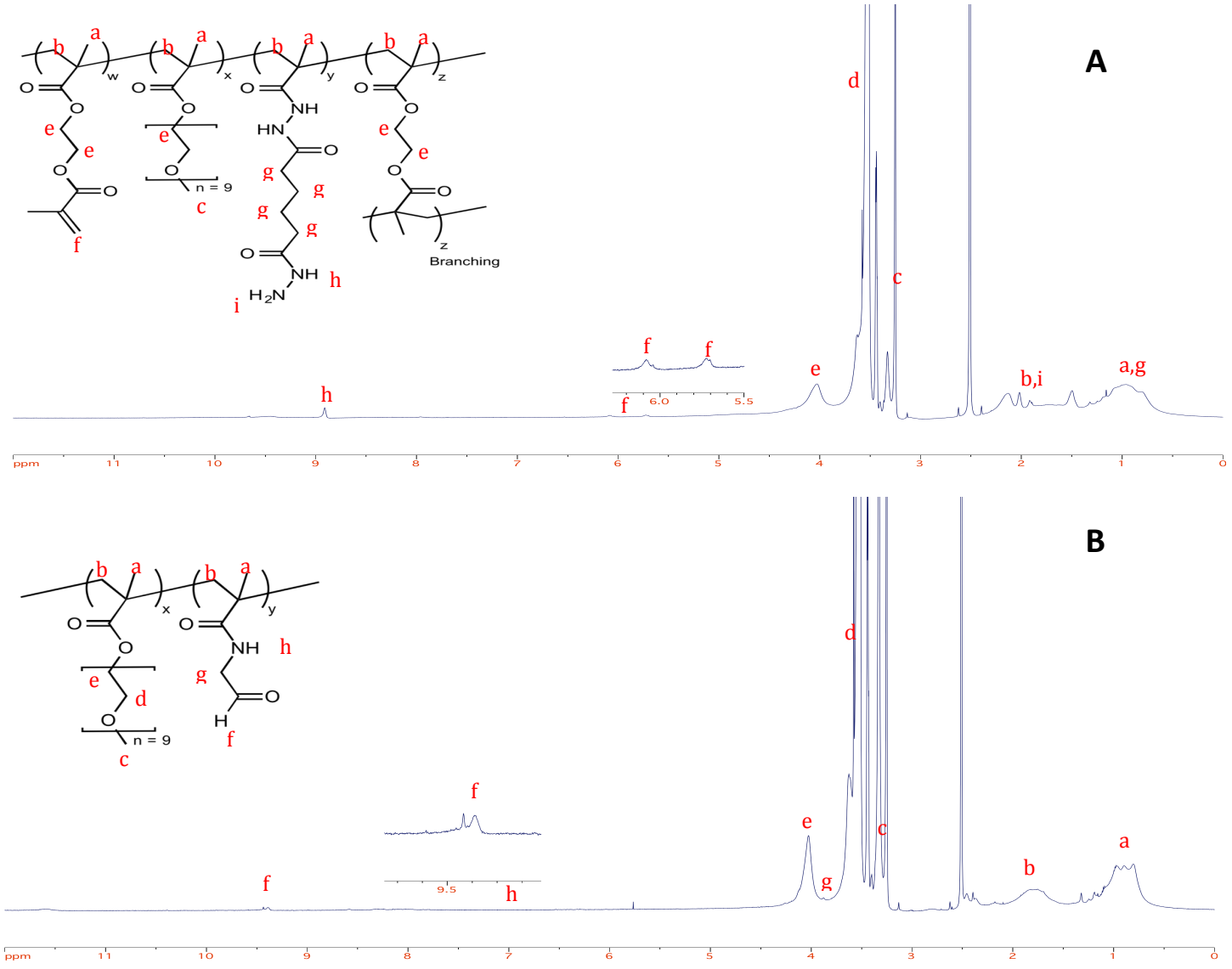

Figure 4 - 2. ^{1}HNMR of (A) PO_{15}-H hyperbranched hydrazide-functionalized POEGMA and (B) PO_{0}-A linear aldehyde-functionalized POEGMA in DMSO at 600 MHz.

Over the time frame of the reactions, the monomer conversions in each of the hyperbranched polymers PO_{15} – PO_5, conversion were roughly similar, ranging from 81% for PO_5 to 83% for P_{15} (Fig. 4 – 3A, Table 4 – 2); however, monomer conversion in the polymerization of linear PO_0 (prepared without EGDMA) was significantly lower (67%) over the same time period. We anticipate this difference is related to the CPCDB transfer constant for $OEGMA_{475}$ being lower than that of EGDMA due to steric hindrance of the long ethylene glycol sidechains in $OEGMA_{475}$, leading to higher conversions in the presence of EGDMA at each measured time point. Furthermore, the rates of M_n increases and the final M_n observed for each polymer varied significantly with the degree of branching, with hyperbranched polymers containing more EGDMA (i.e. with higher DB values) exhibiting faster molecular weight increases and higher final M_n values (Fig. 4 – 3B). Similarly, the polymer dispersity is also positively correlated to the mole fraction of EGDMA included in the synthesis recipe (Fig. 4 – 3C). While the rate effect is partially attributable to the observed increased rate of conversion observed when the mole fraction of EGDMA in the reactions was increased, the mechanism of hyperbranched polymer formation is likely the primary driver of this observation. At low conversions, each molecule would grow and branch independently of one another, given the significantly higher diffusibility of the monomers relative to the growing hyperbranched chains; however, as conversion increases (and monomer concentration decreases), the likelihood that a branch point would be formed between two hyperbranched molecules increases, leading to the formation of significantly larger molecules (Fig. 4 – 4). As the amount of cross-linker in the formulation is increased,

more branches and thus residual vinyl groups would be present on the hyperbranched polymers, further increasing the probability of this intermolecular reaction occurring and thus both higher molecular weights and dispersities being measured.

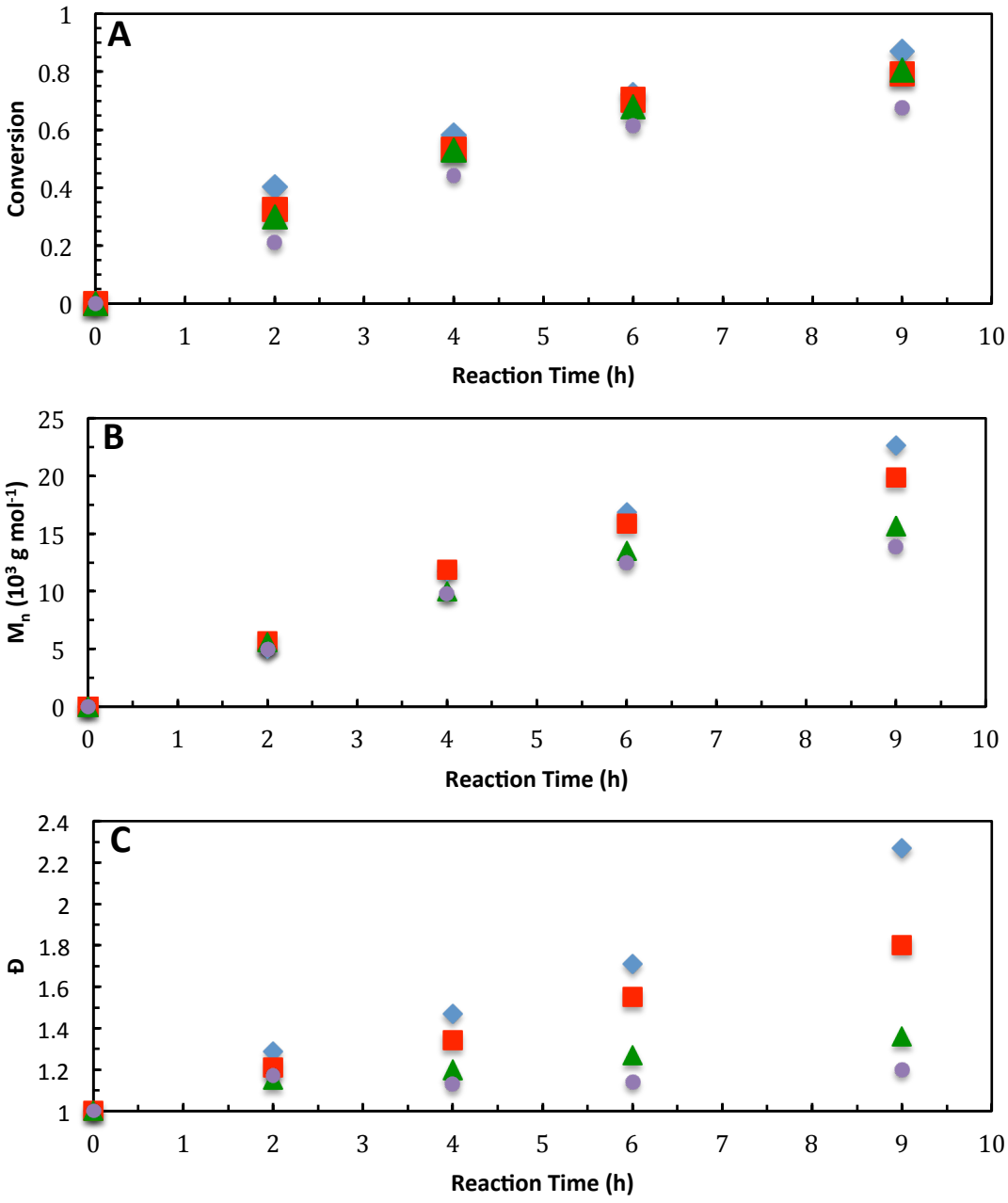

Figure 4 - 3. Polymerization kinetics of PO_{15} (blue diamond), PO_{10} (red square), PO_5 (green triangle), and PO_0 (purple circle) POEGMA polymers over 9 hours at 70 °C. (A) Conversion over time. (B) M_n growth over time as determined by SEC (C) Change in polymer dispersity over time.

The plot of Mn growth as a function of conversion further supports this hypothesis (Fig. 4 – 5). Polymers with lower mole fractions of cross-linker (PO_0 and PO_5) grow in a linear fashion throughout the time course of the reaction, as is typical in a controlled radical polymerization. Polymers with higher mole fractions of cross-linker (PO_{10} – PO_{15}) grow linearly at low conversions, and have lower molecular weights than their linear counterparts at equivalent conversions below 40 – 50%. We hypothesize that this may be due to the formation of intramolecular cross-links that would occur in the growing polymer chains of more highly branched systems. These cross-links would lead to a reduction in the hydrodynamic radius of the more highly branched polymers. As the polymerization proceeded, intermolecular cross-links would begin to occur with greater frequency in the more highly branched systems, leading to a rapid growth in the molecular weight of these systems.

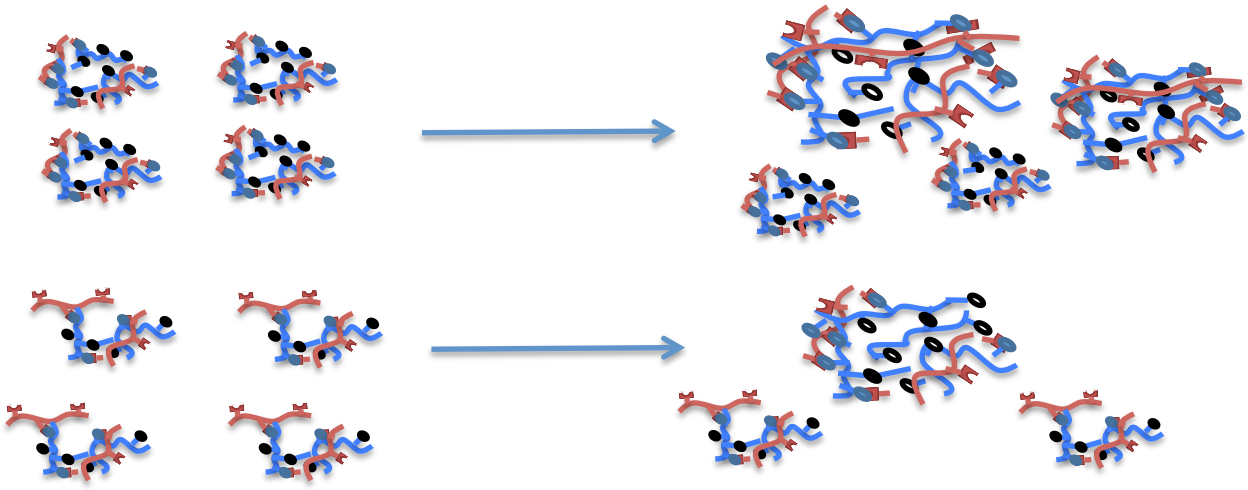

Figure 4 - 4. Schematic representation of the growth of hyperbranched polymers in systems with a higher mole fraction of cross-linker (upper scheme), and lower mole fraction of cross-linker (lower scheme).

Functionalization of the PO_{15}-H - PO_0-H polymers proceeded to ~50% grafting of available MAA groups, yielding functional polymers with approximately 13 – 16 mol% of total monomer residues containing a hydrazide group (Table 4 – 3); no significant difference in functionalization efficiency was noted as a function of the DB. The functionalization of PO_0-A was somewhat less efficient, with 33% conversion of MAA residues observed corresponding to 10 mol% of total monomer residues functionalized with aldehyde groups. We hypothesize the lower conversion in the aldehyde polymers is related to the reduced efficiency of EDC functionalization in organic solvent and/or non-stoichiometric deprotection of the acetal groups to aldehyde groups (Table 4 – 3).

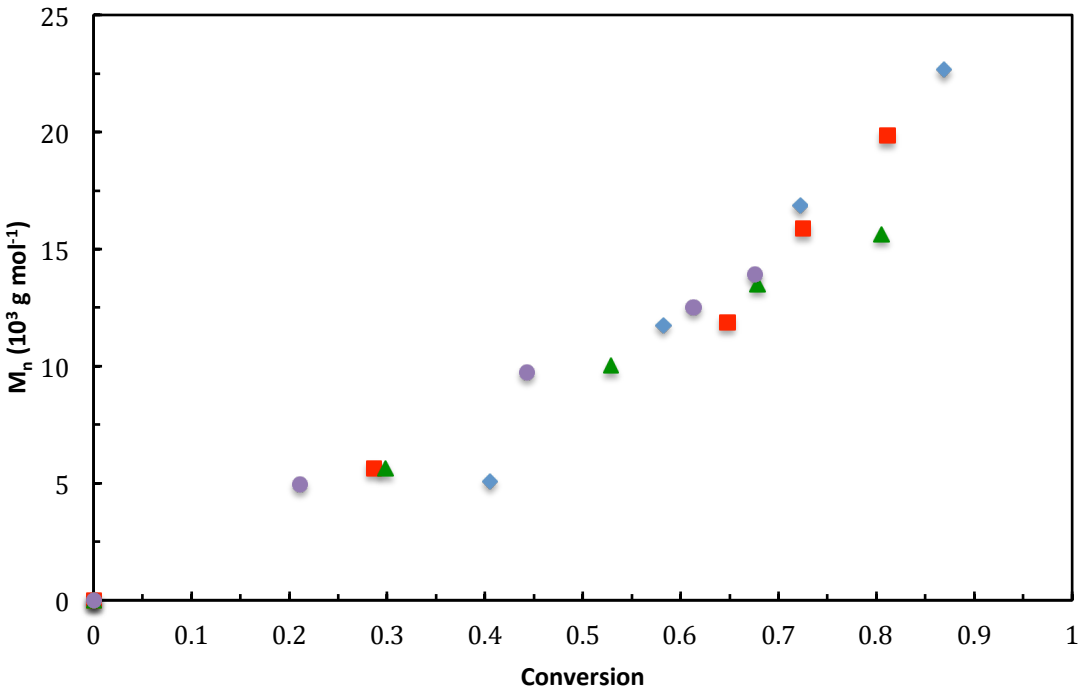

Figure 4 - 5. Growth of number average molecular weight as a function of conversion over the course of a 9 hour polymerization for PO_{15} (blue diamond), PO_{10} (red square), PO_5 (green triangle), and PO_0 (purple circle).

Table 4 - 3. Chemical composition of hydrazide-functionalized hyperbranched polymers and aldehyde-functionalized linear polymers produced by controlled radical polymerization.

Polymer	$OEGMA_{475}$ (mol%)	EGDMA (mol%)	MAA (mol%)	DB (%)	% MAA Residues Functionalized (mol%)	% Residues (Total) With Crosslinkable Group (mol%)
PO_{15}-H	57	17	26	13	50	13
PO_{10}-H	58	13	29	9	52	15
PO_5-H	67	7	26	4	54	14
PO_0-H	70	0	30	0	53	16
PO_0-A	70	0	30	0	33	10

4.3.2 Preparation of injectable hyperbranched/linear POEGMA hybrid hydrogels

A series of four POEGMA hydrogels was prepared by mixing equal volumes of one of the hydrazide-functionalized PO_{15}-H – PO_0-H precursors with the linear aldehyde-functionalized PO_0-A precursor (both at 20 wt%, Table 4 – 4) in a silicone rubber mold (r = 9 mm, v = 240 µl) . All of the polymers were able to successfully form gels *in situ* over the course of approximately 30 minutes (Fig. 4 – 6).

Table 4 - 4. Preparation of injectable POEGMA hydrogels from linear/hyperbranched functionalized precursors.

Gel	Composite Polymers	$[P_n]/[P_{Ald}]$ (mg ml^{-1})	Gelation
G_{15}	PO_{15}-H/PO_0-A	200/200	Y
G_{10}	PO_{10}-H /PO_0-A	200/200	Y
G_5	PO_5-H /PO_0-A	200/200	Y
G_0	PO_0-H /PO_0-A	200/200	Y

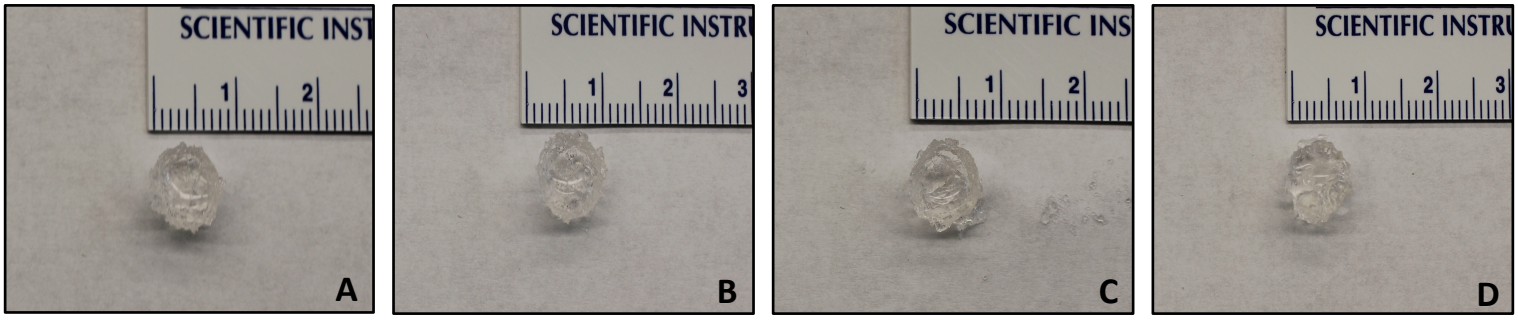

Figure 4 - 6. Images of G_{15} (A), G_{10} (B), G_5 (C), and G_0 (D) gels formed *in situ* by mixing of the relevent PO_n-H hyperbranched/linear hydrazi precursor with the linear PO_0-A aldehyde precursor.

4.3.3 *In vitro* cytotoxicity of hyperbranched/linear POEGMA precursors

The cytotoxicities of the PO_{15} – PO_0-H and PO_0-A polymers were assessed using a resazurin assay on 3T3 mouse fibroblasts. None of the polymers exhibited significant cytotoxicity (Fig. 4 – 7), even up to concentrations of 2 mg ml^{-1} that represents an extremely high concentration in the context of an *in vitro* cytotoxicity assay [90].

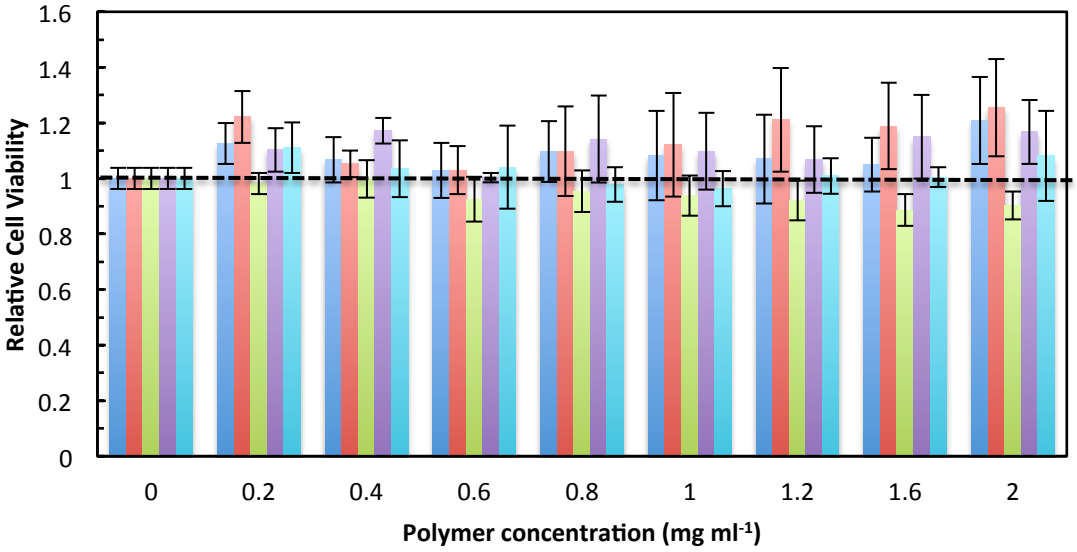

Figure 4 - 7. Relative viability of 3T3 mouse fibroblasts treated with PO_0-H (dark blue), PO_5-H (red), PO_{10}-H (green), PO_{15}-H (purple), and PO_0-A (light blue) for 24 hours at concentrations ranging from 0.2 to 2 mg ml^{-1}. Error bars represent one standard deviation from the mean (n = 3).

4.4 Conclusions and Future Work

A series of four hyperbranched/linear POEGMA polymers with targeted degrees of branching ranging from 0 – 15 mol% were prepared using RAFT polymerization. The measured degrees of branching closely matched the mole fraction of cross-linker added to each polymerization reaction, indicating effective incorporation of cross-links in the hyperbranched polymers. The polymers in the series were shown to be chemically similar, apart from the variation in the mole fraction of cross-linker that was incorporated in each polymer. The rate of molecular weight development over time, the conversion of monomers over the course of the reaction, the size of the polymers, and the dispersity of the final polymer products were all positively correlated with the mole fraction of cross-linker added to the polymerization, consistent with the higher

probability of intermolecular cross-link formation between growing POEGMA macromolecules as the EGDMA content is increased. Furthermore, Mn grew linearly with respect to conversion, indicating that polymerizations proceeded in a controlled manner. All four polymers in the series were successfully functionalized with hydrazide groups, and functionalization proceeded with similar efficiency independent of the degree of branching. When dissolved in solution and mixed with aldehyde-functionalized linear POEGMA, all of the polymers successfully form hydrogels *in situ* within ~30s. An *in vitro* cytotoxicity test indicated that none of the polymers had significant cytotoxic effects, even at relatively high concentrations

Future work will focus on investigating how the degree of branching of polymeric hydrogel precursors affects hydrogel properties, particularly focused on the correlation between the branching of the precursor polymers and the mechanical strength, gelation kinetics, swelling/ degradation rates, etc. of the resulting gels. Additionally, the capacity of these gels to load and release drugs will be assessed, in order to better understand how hyperbranched molecular architecture can be used to modulate rates of drug release from gel-based drug delivery vehicles. Finally, a series of aldehyde functionalized hyperbranched polymers will also be prepared, in order to create *in situ* gelling hydrogels by mixing of hyperbranched/hyperbranched polymer precursors. Attempts at producing these polymers to-date have been unsuccseful due to solubility issues with the final product. The polymerization and functionalization procedures for producing these polymers will have to be optimized in order to overcome these challenges. Ultimately, the gels that are produced from these hyperbranched/hyperbanched

precursors will be investigated in order to determine how the properties of these homogenous gels compare to hybrid hyperbranched/linear and linear/linear injectable gels.

5 Conclusions

5.1 Summary of contributions

Injectable hydrogels were prepared from functionalized POEGMA polymers with a variety of physical characteristics. In particular, both the molecular weight of the polymers and their 3-dimensional structure were systematically varied in order to better understand how these factors affect the properties of hydrogels made from these precursors, as well as the properties of the precursors themselves.

In the former case, a series of five POEGMA polymers were prepared with a range of molecular weights (M_n = 6.7 – 15.9 **kDa**) and narrow dispersities (Đ < 1.3) using RAFT polymerization techniques. The polymers were shown to have similar mole fractions of $OEGMA_{475}$, $M(EO)_2MA$ and MAA, indicating that they were chemically similar, differing only in the concentration of chain transfer agent that was distributed among them. The polymers were successfully functionalized with either hydrazide or aldehyde groups in similar proportions (≈15 and 10 mol% respectively). When dissolved in aqueous solution these polymers were able to rapidly form gels *in situ* by simple mixing of hydrazide and aldehyde-functionalized precursors. A series of four gels was prepared by mixing one of the hydrazide precursors with the aldehyde precursor. A residual functional group assay showed that there were no significant differences in the number of residual functional groups remaining in any of the gels in the series ($p > 0.05$); given that the precursors had similar functional group distributions, this result indicates that cross-links formed at similar densities amongst all of the POEGMA

hydrogels. Variations in the properties of these gels could therefore be attributed to the molecular weight of the POEGMA precursors alone. The gels that were produced using different molecular weight precursors gelled *in situ* over different time periods (15 – 35 s), degraded at different rates in 10 mM HCl (135 – 210 min) at physiological temperature and in 10 mM PBS at room temperature (192 - > 336 h), and had different average shear storage (4.5 – 8.6 kPa) and compressive moduli (14.5 – 29.8 kPa). Additionally, all of the polymers were shown to not be significantly cytotoxic. Ultimately, these results established the viability of using precursor molecular weight to modulate the properties of *in situ* gelling injectable hydrogels made from synthetic polymers. This system has the advantage of allowing control over the physical characteristics of hydrogels without the need to modify their chemical characteristics, allowing for more precise control of the functionality of this biomaterial in tissue engineering and drug delivery contexts.

Similar hydrazone chemistry was applied to prepare injectable hydrogels based on POEGMA precursor polymers with different 3-dimensional architectures, specifically by introducing various degrees of branching into the system. A series of four hyperbranched/ linear polymers were prepared from $OEGMA_{475}$, MAA, and various mole fractions of EGDMA cross-linker (0 – 15%). Measured degrees of branching closely matched the mole fraction of EGDMA cross-linker added in each polymerization recipe, indicating effective incorporation of branches into the POEGMA polymers. Properties of the polymers and of the polymerization reactions varied systematically with the mole fraction of EGDMA (and thus the degree of branching) used to prepare the

hyperbranched polymers, with monomer conversion (from 67 – 84%), molecular weight (M_n= 13.9 – 22.6 **kDa**), and dispersity (Đ = 1.2 – 2.27) all increased with increasing EGDMA mole fraction. The polymers in this series were successfully functionalized with hydrazide groups (approximately 15 mol% incorporation relative to the total number of monomer residues present), with functionalization proceeding with similar efficiency across the series. When mixed with a linear aldehyde-functionalized POEGMA polymer, all of the polymers were able to form hydrogels *in situ*.

5.2 Future work

5.2.1 Future work in tuning the properties of injectable POEGMA hydrogels by controlling precursor polymer molecular weight

Future work will focus on investigating how certain types of cells (particularly stem cells) behave when seeded on or in the aforementioned material. Particular attention will be focused on determining how the physical characteristics of the POEGMA hydrogels can be tuned to direct the growth and differentiation of cells in both *in vitro* and *in vivo* contexts without the confounding effects of different chemical functionalization that are consistently observed in other chemistries used for such investigations. *In vivo* studies will investigate how animal models will respond to hydrogels made from precursors with various molecular weights. The different physical properties of the hydrogels could produce a wide range of responses in different *in vivo* environments (i.e. in bone tissue vs in muscle tissue). Furthermore, the molecular weight of a molecule is a characteristic that is used by some cells in the body to

determine how these cells will interact with that molecule (i.e. whether that molecule will be taken up into the cell, will that molecule pass through junctions in layers of the epithelium); therefore, it is possible that precursors of different sizes will undergo different rates of compartmentalization in and clearance from various *in vivo* environments. Ultimately, results from this study may indicate how precursor molecular weight can be used to optimize POEGMA materials for functions such as drug delivery in different tissues. Additionally, the molecular weight of the aldehyde polymer could be varied as well, to determine how different combinations of aldehyde/hydrazide precursors with various molecular weights affect hydrogel properties.

5.2.2 Future work in controlled synthesis of A/B functionalized hyperbranched POEGMA polymers for use in the preparation of injectable hydrogels

Future work will focus on investigating how the degree of branching of these hydrogel precursor polymers affects the properties of the hydrogels that they form. The results of this study should provide information on how the 3-dimensional structure (and branching in particular) of a polymer precursor can be manipulated to tune the properties of injectable hydrogels, which is a method for modulating the properties of hydrogels that has not been extensively explored to-date. Hyperbranched architecture in polymer precursors could affect such gel properties as mechanical strength in different dimensions or the cellular response to the material. Studies will also be undertaken to determine how hyperbranching in polymer precursors affects drug loading and release from injectable hydrogels. Because the hyperbranched regions within these types of hydrogels are formed via different types of covalent cross-links

than those that are formed between hydrazide/aldehyde groups, they may affect how different types of drugs are partitioned within the hydrogel, as well as the rate of drug release due to degradation of the bulk hydrogel. In particular, a study will be undertaken to produce hyperbranched polymers from short-chain POEGMA (which has a significantly lower transition temperature than long chain POEGMA). This should result in hydrogels with hydrophobic domains of various sizes, which should produce interesting effects in the context of the loading and delivery of hydrophobic drugs. Additionally, the size of the hyperbranched polymer could be varied while the degree of branching is kept constant, in order to study how increasing or decreasing the volume of hyperbranched regions within a gel affects gel proeprties. Finally, aldehyde-functionalized hyperbranched polymers will be produced as well, in order to form gels from the *in situ* mixing of only hyperbranched precursors. These gels will be studied to determine if they exhibit different/preferable properties when compared to hybrid hydrogels produced from linear/hyperbranched precursors, as well as gels produced from linear/linear precursors.

References

[1] Calo E, Khutoryanskiy VV. Biomedical applications of hydrogels: A review of patents and commercial products. Eur Polym J 2015;65:252-67.
[2] Peppas NA, Bures P, Leobandung W, Ichikawa H. Hydrogels in pharmaceutical formulations. Eur J Pharm Biopharm 2000;50:27-46.
[3] Hoare TR, Kohane DS. Hydrogels in drug delivery: Progress and challenges. Polymer 2008;49:1993-2007.
[4] Ashley GW, Henise J, Reid R, Santi DV. Hydrogel drug delivery system with predictable and tunable drug release and degradation rates. P Natl Acad Sci USA 2013;110:2318-23.
[5] Hoffman AS. Hydrogels for biomedical applications. Adv Drug Deliver Rev 2012;64:18-23.
[6] Oddo L, Masci G, Di Meo C, Capitani D, Mannina L, Lamanna R, et al. Novel thermosensitive calcium alginate microspheres: Physico-chemical characterization and delivery properties. Acta Biomater 2010;6:3657-64.
[7] Merino S, Martin C, Kostarelos K, Prato M, Vazquez E. Nanocomposite Hydrogels: 3D Polymer-Nanoparticle Synergies for On-Demand Drug Delivery. Acs Nano 2015;9:4686-97.
[8] Hunt JA, Chen R, van Veen T, Bryan N. Hydrogels for tissue engineering and regenerative medicine. J Mater Chem B 2014;2:5319-38.
[9] Huebsch N, Arany PR, Mao AS, Shvartsman D, Ali OA, Bencherif SA, et al. Harnessing traction-mediated manipulation of the cell/matrix interface to control stem-cell fate. Nature Materials 2010;9:518-26.
[10] Gilbert PM, Havenstrite KL, Magnusson KEG, Sacco A, Leonardi NA, Kraft P, et al. Substrate Elasticity Regulates Skeletal Muscle Stem Cell Self-Renewal in Culture. Science 2010;329:1078-81.
[11] Benoit DSW, Durney AR, Anseth KS. The effect of heparin-functionalized PEG hydrogels on three-dimensional human mesenchymal stem cell osteogenic differentiation. Biomaterials 2007;28:66-77.
[12] Zhang B, Montgomery M, Chamberlain MD, Ogawa S, Korolj A, Pahnke A, et al. Biodegradable scaffold with built-in vasculature for organ-on-a-chip engineering and direct surgical anastomosis. Nat Mater 2016.
[13] Ma L, Barker J, Zhou CC, Li W, Zhang J, Lin BY, et al. Towards personalized medicine with a three-dimensional micro-scale perfusion-based two-chamber tissue model system. Biomaterials 2012;33:4353-61.
[14] Bidarra SJ, Barrias CC, Granja PL. Injectable alginate hydrogels for cell delivery in tissue engineering. Acta Biomater 2014;10:1646-62.
[15] Seol YJ, Park JY, Jeong W, Kim TH, Kim SY, Cho DW. Development of hybrid scaffolds using ceramic and hydrogel for articular cartilage tissue regeneration. J Biomed Mater Res A 2015;103:1404-13.

[16] Wang DA, Varghese S, Sharma B, Strehin I, Fermanian S, Gorham J, et al. Multifunctional chondroitin sulphate for cartilage tissue-biomaterial integration. Nat Mater 2007;6:385-92.
[17] Sharma R, Pathak K. Polymeric nanosponges as an alternative carrier for improved retention of econazole nitrate onto the skin through topical hydrogel formulation. Pharm Dev Technol 2011;16:367-76.
[18] Brennan NA, Coles ML, Comstock TL, Levy B. A 1-year prospective clinical trial of balafilcon a (PureVision) silicone-hydrogel contact lenses used on a 30-day continuous wear schedule. Ophthalmology 2002;109:1172-7.
[19] Tan H, Rubin JP, Marra KG. Injectable in situ forming biodegradable chitosan-hyaluronic acid based hydrogels for adipose tissue regeneration. Organogenesis 2010;6:173-80.
[20] Yu L, Ding J. Injectable hydrogels as unique biomedical materials. Chem Soc Rev 2008;37:1473-81.
[21] Van Tomme SR, Storm G, Hennink WE. In situ gelling hydrogels for pharmaceutical and biomedical applications. International Journal of Pharmaceutics 2008;355:1-18.
[22] Patenaude M, Smeets NM, Hoare T. Designing injectable, covalently cross-linked hydrogels for biomedical applications. Macromol Rapid Commun 2014;35:598-617.
[23] Longmire M, Choyke PL, Kobayashi H. Clearance properties of nano-sized particles and molecules as imaging agents: considerations and caveats. Nanomedicine (Lond) 2008;3:703-17.
[24] Yu YX, Deng C, Meng FH, Shi Q, Feijen J, Zhong ZY. Novel injectable biodegradable glycol chitosan-based hydrogels crosslinked by Michael-type addition reaction with oligo(acryloyl carbonate)-b-poly(ethylene glycol)-b-oligo(acryloyl carbonate) copolymers. Journal of Biomedical Materials Research Part A 2011;99a:316-26.
[25] Samanta S, Nath B, Baruah JB. Hydrolytically stable Schiff base as highly sensitive aluminium sensor. Inorg Chem Commun 2012;22:98-100.
[26] Garver JM, Gronert S, Bierbaum VM. Experimental Validation of the alpha-Effect in the Gas Phase. J Am Chem Soc 2011;133:13894-7.
[27] Garrod S, Bollard ME, Nicholls AW, Connor SC, Connelly J, Nicholson JK, et al. Integrated metabonomic analysis of the multiorgan effects of hydrazine toxicity in the rat. Chem Res Toxicol 2005;18:115-22.
[28] Vetrik M, Pradny M, Hruby M, Michalek J. Hydrazone-based hydrogel hydrolytically degradable in acidic environment. Polym Degrad Stabil 2011;96:756-9.
[29] Kale AA, Torchilin VP. Design, synthesis, and characterization of pH-sensitive PEG-PE conjugates for stimuli-sensitive pharmaceutical nanocarriers: The effect of substitutes at the hydrazone linkage on the pH stability of PEG-PE conjugates. Bioconjugate Chem 2007;18:363-70.
[30] Zhang R, Huang ZB, Xue MY, Yang J, Tan TW. Detailed characterization of an injectable hyaluronic acid-polyaspartylhydrazide hydrogel for protein delivery. Carbohyd Polym 2011;85:717-25.

[31] Dahlmann J, Krause A, Moller L, Kensah G, Mowes M, Diekmann A, et al. Fully defined in situ cross-linkable alginate and hyaluronic acid hydrogels for myocardial tissue engineering. Biomaterials 2013;34:940-51.
[32] Ito T, Yeo Y, Highley CB, Bellas E, Kohane DS. Dextran-based in situ cross-linked injectable hydrogels to prevent peritoneal adhesions. Biomaterials 2007;28:3418-26.
[33] Luo Y, Kobler JB, Heaton JT, Jia X, Zeitels SM, Langer R. Injectable hyaluronic acid-dextran hydrogels and effects of implantation in ferret vocal fold. J Biomed Mater Res B Appl Biomater 2010;93:386-93.
[34] Martinez-Sanz E, Ossipov DA, Hilborn J, Larsson S, Jonsson KB, Varghese OP. Bone reservoir: Injectable hyaluronic acid hydrogel for minimal invasive bone augmentation. J Control Release 2011;152:232-40.
[35] Patenaude M, Hoare T. Injectable, Degradable Thermoresponsive Poly(N-isopropylacrylamide) Hydrogels. Acs Macro Lett 2012;1:409-13.
[36] Smeets NMB, Bakaic E, Patenaude M, Hoare T. Injectable and tunable poly(ethylene glycol) analogue hydrogels based on poly(oligoethylene glycol methacrylate). Chem Commun 2014;50:3306-9.
[37] Lin CC, Anseth KS. PEG hydrogels for the controlled release of biomolecules in regenerative medicine. Pharm Res 2009;26:631-43.
[38] Zanini S, Muller M, Riccardi C, Orlandi M. Polyethylene glycol grafting on polypropylene membranes for anti-fouling properties. Plasma Chem Plasma P 2007;27:446-57.
[39] Feng LZ, Yang XZ, Shi XZ, Tan XF, Peng R, Wang J, et al. Polyethylene Glycol and Polyethylenimine Dual-Functionalized Nano-Graphene Oxide for Photothermally Enhanced Gene Delivery. Small 2013;9:1989-97.
[40] Ruan JL, Tulloch NL, Muskheli V, Genova EE, Mariner PD, Anseth KS, et al. An improved cryosection method for polyethylene glycol hydrogels used in tissue engineering. Tissue Eng Part C Methods 2013;19:794-801.
[41] Cole AJ, David AE, Wang J, Galban CJ, Hill HL, Yang VC. Polyethylene glycol modified, cross-linked starch-coated iron oxide nanoparticles for enhanced magnetic tumor targeting. Biomaterials 2011;32:2183-93.
[42] McCall JD, Anseth KS. Thiol-ene photopolymerizations provide a facile method to encapsulate proteins and maintain their bioactivity. Biomacromolecules 2012;13:2410-7.
[43] Farrugia BL, Kempe K, Schubert US, Hoogenboom R, Dargaville TR. Poly(2-oxazoline) hydrogels for controlled fibroblast attachment. Biomacromolecules 2013;14:2724-32.
[44] Lutz JF, Andrieu J, Uzgun S, Rudolph C, Agarwal S. Biocompatible, thermoresponsive, and biodegradable: Simple preparation of "all-in-one" biorelevant polymers. Macromolecules 2007;40:8540-3.
[45] Ling YY, Ren J, Li T, Zhao YB, Wu CL. POEGMA-based disulfide-containing fluorescent probes for imitating and tracing noninternalization-based intracellular drug delivery. Chem Commun 2016;52:4533-6.

[46] Huang R, Ferhan AR, Guo LH, Qiu B, Lin ZY, Kim DH, et al. In situ synthesis of protein-resistant poly(oligo(ethylene glycol)methacrylate) films in capillary for protein separation. Rsc Adv 2014;4:4883-8.
[47] Wang HY, Feng YK, An B, Zhang WC, Sun ML, Fang ZC, et al. Fabrication of PU/PEGMA crosslinked hybrid scaffolds by in situ UV photopolymerization favoring human endothelial cells growth for vascular tissue engineering. J Mater Sci-Mater M 2012;23:1499-510.
[48] Lutz JF, Hoth A. Preparation of ideal PEG analogues with a tunable thermosensitivity by controlled radical copolymerization of 2-(2-methoxyethoxy)ethyl methacrylate and oligo(ethylene glycol) methacrylate. Macromolecules 2006;39:893-6.
[49] Smeets NM, Bakaic E, Patenaude M, Hoare T. Injectable poly(oligoethylene glycol methacrylate)-based hydrogels with tunable phase transition behaviours: physicochemical and biological responses. Acta Biomater 2014;10:4143-55.
[50] Xu F, Sheardown H, Hoare T. Reactive electrospinning of degradable poly(oligoethylene glycol methacrylate)-based nanofibrous hydrogel networks. Chem Commun 2016;52:1451-4.
[51] Deng XD, Smeets NMB, Sicard C, Wang JY, Brennan JD, Filipe CDM, et al. Poly(oligoethylene glycol methacrylate) Dip-Coating: Turning Cellulose Paper into a Protein-Repellent Platform for Biosensors. J Am Chem Soc 2014;136:12852-5.
[52] Braun D. Polymer synthesis : theory and practice : fundamentals, methods, experiments. 4th ed. Berlin ; New York: Springer; 2005.
[53] Miyakoshi R, Yokoyama A, Yokozawa T. Development of catalyst-transfer condensation polymerization. Synthesis of pi-conjugated polymers with controlled molecular weight and low polydispersity. J Polym Sci Pol Chem 2008;46:753-65.
[54] Matyjaszewski K. Atom Transfer Radical Polymerization (ATRP): Current Status and Future Perspectives. Macromolecules 2012;45:4015-39.
[55] Chanda M. Introduction to polymer science and chemistry : a problem-solving approach. Second edition. ed. Boca Raton: CRC Press, Taylor & Francis Group; 2013.
[56] Chiefari J, Chong YK, Ercole F, Krstina J, Jeffery J, Le TPT, et al. Living free-radical polymerization by reversible addition-fragmentation chain transfer: The RAFT process. Macromolecules 1998;31:5559-62.
[57] Moad G, Rizzardo E, Thang SH. Living Radical Polymerization by the RAFT Process - A Second Update. Aust J Chem 2009;62:1402-72.
[58] Luzon M, Boyer C, Peinado C, Corrales T, Whittaker M, Tao L, et al. Water-Soluble, Thermoresponsive, Hyperbranched Copolymers Based on PEG-Methacrylates: Synthesis, Characterization, and LCST Behavior. J Polym Sci Pol Chem 2010;48:2783-92.
[59] Semsarilar M, Perrier S. 'Green' reversible addition-fragmentation chain-transfer (RAFT) polymerization. Nat Chem 2010;2:811-20.
[60] Warren NJ, Armes SP. Polymerization-Induced Self-Assembly of Block Copolymer Nano-objects via RAFT Aqueous Dispersion Polymerization. J Am Chem Soc 2014;136:10174-85.

[61] Chong JYT, Mulet X, Postma A, Keddie DJ, Waddington LJ, Boyd BJ, et al. Novel RAFT amphiphilic brush copolymer steric stabilisers for cubosomes: poly(octadecyl acrylate)-block-poly(polyethylene glycol methyl ether acrylate). Soft Matter 2014;10:6666-76.
[62] Nehache S, Yeh CC, Semsarilar M, Deratani A, Chang Y, Quemener D. Anti-Bioadhesive Coating Based on Easy to Make Pseudozwitterionic RAFT Block Copolymers for Blood-Contacting Applications. Macromol Biosci 2016;16:57-62.
[63] Dalnoki-Veress K, Forrest JA, Murray C, Gigault C, Dutcher JR. Molecular weight dependence of reductions in the glass transition temperature of thin, freely standing polymer films. Phys Rev E 2001;63.
[64] Kasaai MR, Arul J, Charlet C. Intrinsic viscosity-molecular weight relationship for chitosan. J Polym Sci Pol Phys 2000;38:2591-8.
[65] Huang M, Khor E, Lim LY. Uptake and cytotoxicity of chitosan molecules and nanoparticles: Effects of molecular weight and degree of deacetylation. Pharmaceutical Research 2004;21:344-53.
[66] Choi HS, Liu W, Misra P, Tanaka E, Zimmer JP, Ipe BI, et al. Renal clearance of quantum dots. Nat Biotechnol 2007;25:1165-70.
[67] Temenoff JS, Athanasiou KA, LeBaron RG, Mikos AG. Effect of poly(ethylene glycol) molecular weight on tensile and swelling properties of oligo(poly(ethylene glycol) fumarate) hydrogels for cartilage tissue engineering. J Biomed Mater Res 2002;59:429-37.
[68] Zhou HY, Chen XG, Kong M, Liu CS, Cha DS, Kennedy JF. Effect of molecular weight and degree of chitosan deacetylation on the preparation and characteristics of chitosan thermosensitive hydrogel as a delivery system. Carbohyd Polym 2008;73:265-73.
[69] Rosso F, Giordano A, Barbarisi M, Barbarisi A. From cell-ECM interactions to tissue engineering. J Cell Physiol 2004;199:174-80.
[70] Ishida Y, Jikei M, Kakimoto M. Synthesis of hyperbranched aromatic polyesters by carbon monoxide insertion reaction using palladium catalyst. Polym Advan Technol 2000;11:698-704.
[71] Abbasi E, Aval SF, Akbarzadeh A, Milani M, Nasrabadi HT, Joo SW, et al. Dendrimers: synthesis, applications, and properties. Nanoscale Res Lett 2014;9.
[72] Tomalia DA, Frechet JMJ. Discovery of dendrimers and dendritic polymers: A brief historical perspective. J Polym Sci Pol Chem 2002;40:2719-28.
[73] Fu HL, Cheng SX, Zhang XZ, Zhuo RX. Dendrimer/DNA complexes encapsulated functional biodegradable polymer for substrate-mediated gene delivery. J Gene Med 2008;10:1334-42.
[74] Kojima C, Turkbey B, Ogawa M, Bernardo M, Regino CAS, Bryant LH, et al. Dendrimer-based MRI contrast agents: the effects of PEGylation on relaxivity and pharmacokinetics. Nanomed-Nanotechnol 2011;7:1001-8.
[75] Zheng YC, Li SP, Weng ZL, Gao C. Hyperbranched polymers: advances from synthesis to applications. Chemical Society Reviews 2015;44:4091-130.
[76] Yan D, Gao C, Frey H. Hyperbranched polymers : synthesis, properties, and applications. Hoboken: Wiley; 2011.

[77] Svenson S. The dendrimer paradox--high medical expectations but poor clinical translation. Chem Soc Rev 2015;44:4131-44.
[78] Liu JY, Pang Y, Chen J, Huang P, Huang W, Zhu XY, et al. Hyperbranched polydiselenide as a self assembling broad spectrum anticancer agent. Biomaterials 2012;33:7765-74.
[79] Asri LATW, Crismaru M, Roest S, Chen Y, Ivashenko O, Rudolf P, et al. A Shape-Adaptive, Antibacterial- Coating of Immobilized Quaternary- Ammonium Compounds Tethered on Hyperbranched Polyurea and its Mechanism of Action. Adv Funct Mater 2014;24:346-55.
[80] Nair LS, Laurencin CT. Biodegradable polymers as biomaterials. Prog Polym Sci 2007;32:762-98.
[81] Tian HY, Tang ZH, Zhuang XL, Chen XS, Jing XB. Biodegradable synthetic polymers: Preparation, functionalization and biomedical application. Prog Polym Sci 2012;37:237-80.
[82] Hu ZB, Cai T, Chi CL. Thermoresponsive oligo(ethylene glycol)-methacrylate- based polymers and microgels. Soft Matter 2010;6:2115-23.
[83] Tao L, Mantovani G, Lecolley F, Haddleton DM. alpha-aldehyde terminally functional methacrylic polymers from living radical polymerization: Application in protein conjugation "pegylation". J Am Chem Soc 2004;126:13220-1.
[84] Viswanathan P, Themistou E, Ngamkham K, Reilly GC, Armes SP, Battaglia G. Controlling Surface Topology and Functionality of Electrospun Fibers on the Nanoscale using Amphiphilic Block Copolymers To Direct Mesenchymal Progenitor Cell Adhesion. Biomacromolecules 2015;16:66-75.
[85] Fechler N, Badi N, Schade K, Pfeifer S, Lutz JF. Thermogelation of PEG-Based Macromolecules of Controlled Architecture. Macromolecules 2009;42:33-6.
[86] Lei J, Mayer C, Freger V, Ulbricht M. Synthesis and Characterization of Poly(ethylene glycol) Methacrylate Based Hydrogel Networks for Anti-Biofouling Applications. Macromol Mater Eng 2013;298:967-80.
[87] Yoon JA, Kowalewski T, Matyjaszewski K. Comparison of Thermoresponsive Deswelling Kinetics of Poly(oligo(ethylene oxide) methacrylate)-Based Thermoresponsive Hydrogels Prepared by "Graft-from" ATRP. Macromolecules 2011;44:2261-8.
[88] Bakaic E, Smeets NMB, Dorrington H, Hoare T. "Off-the-shelf" thermoresponsive hydrogel design: tuning hydrogel properties by mixing precursor polymers with different lower-critical solution temperatures. Rsc Adv 2015;5:33364-76.
[89] De France KJ, Chan KJW, Cranston ED, Hoare T. Enhanced Mechanical Properties in Cellulose Nanocrystal-Poly(oligoethylene glycol methacrylate) Injectable Nanocomposite Hydrogels through Control of Physical and Chemical Cross-Linking. Biomacromolecules 2016;17:649-60.
[90] Smeets NMB, Bakaic E, Patenaude M, Hoare T. Injectable poly(oligoethylene glycol methacrylate)-based hydrogels with tunable phase transition behaviours: Physicochemical and biological responses. Acta Biomater 2014;10:4143-55.

[91] Smeets NMB, Patenaude M, Kinio D, Yavitt FM, Bakaic E, Yang FC, et al. Injectable hydrogels with in situ-forming hydrophobic domains: oligo(D,L-lactide) modified poly(oligoethylene glycol methacrylate) hydrogels. Polym Chem-Uk 2014;5:6811-23.
[92] Kong HJ, Kaigler D, Kim K, Mooney DJ. Controlling rigidity and degradation of alginate hydrogels via molecular weight distribution. Biomacromolecules 2004;5:1720-7.
[93] Benoit DSW, Schwartz MP, Durney AR, Anseth KS. Small functional groups for controlled differentiation of hydrogel-encapsulated human mesenchymal stem cells. Nature Materials 2008;7:816-23.
[94] Curran JM, Chen R, Hunt JA. The guidance of human mesenchymal stem cell differentiation in vitro by controlled modifications to the cell substrate. Biomaterials 2006;27:4783-93.
[95] Keselowsky BG, Collard DM, Garcia AJ. Surface chemistry modulates focal adhesion composition and signaling through changes in integrin binding. Biomaterials 2004;25:5947-54.
[96] Perizzolo D, Lacefield WR, Brunette DM. Interaction between topography and coating in the formation of bone nodules in culture for hydroxyapatite- and titanium-coated micromachined surfaces. J Biomed Mater Res 2001;56:494-503.
[97] Fiten MWM, Paulus RM, Schubert US. Systematic parallel investigation of RAFT polymerizations for eight different (meth)acrylates: A basis for the designed synthesis of block and random copolymers. J Polym Sci Pol Chem 2005;43:3831-9.
[98] Hoogenboom R, Schubert US, Van Camp W, Du Prez FE. RAFT polymerization of 1-ethoxyethyl acrylate: A novel route toward near-monodisperse poly(acrylic acid) and derived block copolymer structures. Macromolecules 2005;38:7653-9.
[99] Sridhar R, Pliszka D, Luo HK, Lim KHC, Ramakrishna S. Medical Devices Regulatory Aspects: A Special Focus on Polymeric Material Based Devices. Curr Pharm Design 2015;21:6246-59.
[100] Pasut G, Veronese FM. Polymer-drug conjugation, recent achievements and general strategies. Prog Polym Sci 2007;32:933-61.
[101] Dienstknecht T, Ehehalt K, Jenei-Lanzl Z, Zellner J, Muller M, Berner A, et al. Resazurin dye as a reliable tool for determination of cell number and viability in mesenchymal stem cell culture. Bull Exp Biol Med 2010;150:157-9.
[102] Hernandez-Guerrero M, Stenzel MH. Honeycomb structured polymer films via breath figures. Polym Chem-Uk 2012;3:563-77.
[103] Chin SM, He HK, Konkolewicz D, Matyjaszewski K. Synthesis of Triblock and Multiblock Methacrylate Polymers and Self-Assembly of Stimuli Responsive Triblock Polymers. J Polym Sci Pol Chem 2014;52:2548-55.
[104] Rubinstein M, Colby RH. Polymer physics. Oxford ; New York: Oxford University Press; 2003.
[105] Zhou LJ, Liang D, He XL, Li JH, Tan H, Li JS, et al. The degradation and biocompatibility of pH-sensitive biodegradable polyurethanes for intracellular multifunctional antitumor drug delivery. Biomaterials 2012;33:2734-45.
[106] Higuchi A, Ling QD, Chang Y, Hsu ST, Umezawa A. Physical cues of biomaterials guide stem cell differentiation fate. Chem Rev 2013;113:3297-328.

[107] Kim TH, An DB, Oh SH, Kang MK, Song HH, Lee JH. Creating stiffness gradient polyvinyl alcohol hydrogel using a simple gradual freezing-thawing method to investigate stem cell differentiation behaviors. Biomaterials 2015;40:51-60.
[108] Lee J, Abdeen AA, Zhang D, Kilian KA. Directing stem cell fate on hydrogel substrates by controlling cell geometry, matrix mechanics and adhesion ligand composition. Biomaterials 2013;34:8140-8.
[109] Dong Y, Saeed A, Hassan W, Tai H, Pandit A, Wang W. Thiol-ene clickable PEG based thermoresponsive hyperbranched copolymer for in situ crosslinking hybrid hydrogel. J Tissue Eng Regen M 2012;6:190-1.
[110] Joshi N, Grinstaff M. Applications of dendrimers in tissue engineering. Curr Top Med Chem 2008;8:1225-36.
[111] Mintzer MA, Grinstaff MW. Biomedical applications of dendrimers: a tutorial. Chemical Society Reviews 2011;40:173-90.
[112] Desai PN, Yuan Q, Yang H. Synthesis and Characterization of Photocurable Polyamidoamine Dendrimer Hydrogels as a Versatile Platform for Tissue Engineering and Drug Delivery. Biomacromolecules 2010;11:666-73.
[113] Hassan W, Dong YX, Wang WX. Encapsulation and 3D culture of human adipose-derived stem cells in an in-situ crosslinked hybrid hydrogel composed of PEG-based hyperbranched copolymer and hyaluronic acid. Stem Cell Res Ther 2013;4.
[114] Liu YH, Zhang FH, Ru YY. Hyperbranched phosphoramidate-hyaluronan hybrid: A reduction-sensitive injectable hydrogel for controlled protein release. Carbohyd Polym 2015;117:304-11.
[115] Jin HB, Huang W, Zhu XY, Zhou YF, Yan DY. Biocompatible or biodegradable hyperbranched polymers: from self-assembly to cytomimetic applications. Chemical Society Reviews 2012;41:5986-97.
[116] Isaure F, Cormack PAG, Sherrington DC. Synthesis of branched poly(methyl methacrylate)s: Effect of the branching comonomer structure. Macromolecules 2004;37:2096-105.
[117] O'Brien N, McKee A, Sherrington DC, Slark AT, Titterton A. Facile, versatile and cost effective route to branched vinyl polymers. Polymer 2000;41:6027-31.
[118] Ishizu K, Ohta Y, Kawauchi S. Kinetics of hyperbranched polystyrenes by free radical polymerization of photofunctional inimer. Macromolecules 2002;35:3781-4.
[119] Alfurhood JA, Sun H, Bachler PR, Sumerlin BS. Hyperbranched poly(N-(2-hydroxypropyl)methacrylamide) via RAFT self-condensing vinyl polymerization. Polym Chem-Uk 2016;7:2099-104.
[120] Dong YX, Qin Y, Dubaa M, Killion J, Gao YS, Zhao TY, et al. A rapid crosslinking injectable hydrogel for stem cell delivery, from multifunctional hyperbranched polymers via RAFT homopolymerization of PEGDA. Polym Chem-Uk 2015;6:6182-92.
[121] Tai H, Tochwin A, El-Betany A, Wang W. Degradable and Thermoresponsive Hyperbranched Polymers Synthesized via One-pot RAFT Polymerization for Injectable Scaffolds Applications. Tissue Eng Pt A 2015;21:S54-S.
[122] Dong YX, Saeed AO, Hassan W, Keigher C, Zheng Y, Tai HY, et al. "One-step" Preparation of Thiol-Ene Clickable PEG-Based Thermoresponsive Hyperbranched

Copolymer for In Situ Crosslinking Hybrid Hydrogel. Macromol Rapid Comm 2012;33:120-6.
[123] Kennedy R, Ul Hassan W, Tochwin A, Zhao TY, Dong YX, Wang Q, et al. In situ formed hybrid hydrogels from PEG based multifunctional hyperbranched copolymers: a RAFT approach. Polym Chem-Uk 2014;5:1838-42.

Appendix A1

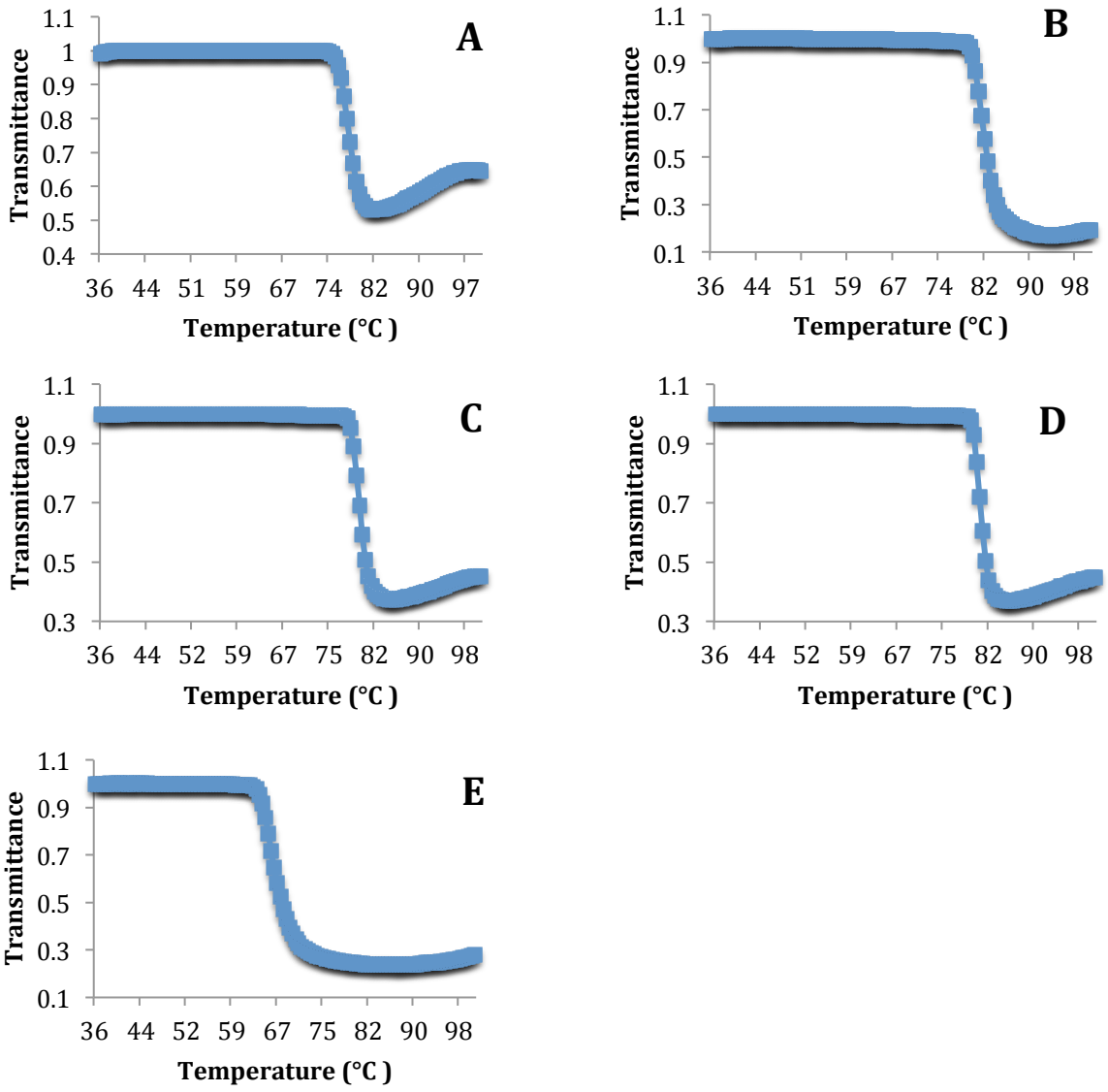

Figure A – 1. Transmittance readings of 5 mg ml^{-1} solutions of $POH_{6.7}$ (A), $POH_{9.3}$ (B), $POH_{11.6}$ (C), $POH_{15.9}$ (D), and $POA_{15.0}$ (E) in 10 mM PBS, as determined by UV-Vis spectroscopy. Readings were taken at 0.5 °C intervals over a temperature ramp from 36 – 100 °C, at a rate of 1 °C min^{-1}.

Appendix A2

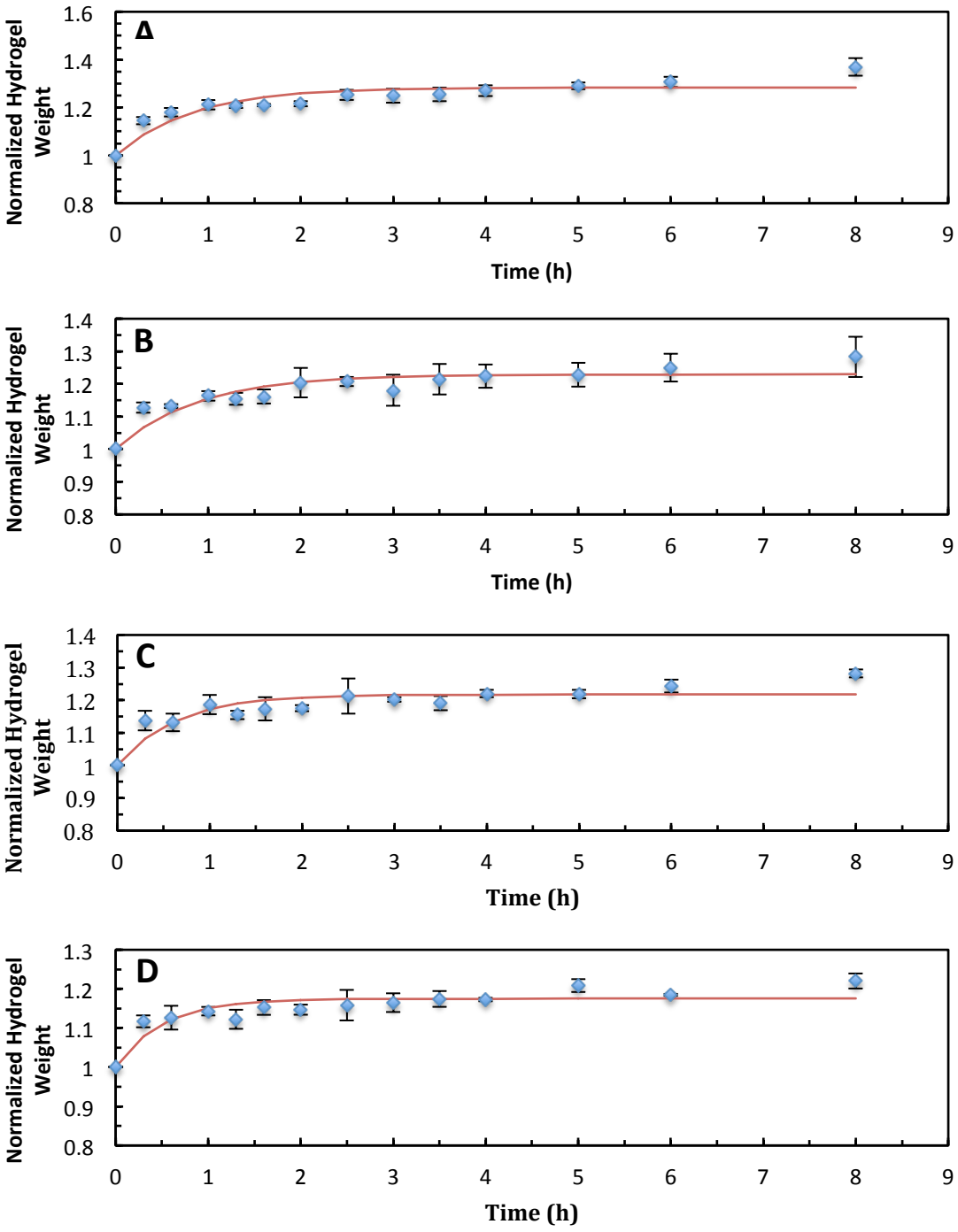

Appendix Figure A2. Swelling of $POH_{6.7}/POA_{15.0}$ (A), $POH_{9.3}/POA_{15.0}$ (B), $POH_{11.6}/POA_{15.0}$ (C), and $POH_{15.9}/POA_{15.0}$ (D) over 8 hours in 10 mM PBS at 22 °C. Markers indicate measured swelling ratios, lines show modeled swelling ratios over the same time period. Error bars represent one standard deviation from the mean (n = 3).